

T.C.
DOKUZ EYLUL UNIVERSITY
IZMIR INTERNATIONAL BIOMEDICINE
AND GENOME INSTITUTE

**THE ROLE OF c-MET ACTIVATION ON THE
ORGAN SPECIFIC EXTRAVASATION IN
HEPATOCELLULAR CARCINOMA CELLS**

GÜLSÜN BAĞCI

MOLECULAR BIOLOGY AND GENETICS

MASTER DISSERTATION

IZMIR-2019

Thesis Code: DEU.İBG.MSc-2016850007

T.C.
DOKUZ EYLUL UNIVERSITY
IZMIR INTERNATIONAL BIOMEDICINE
AND GENOME INSTITUTE

**THE ROLE OF c-MET ACTIVATION ON THE
ORGAN SPECIFIC EXTRAVASATION IN
HEPATOCELLULAR CARCINOMA CELLS**

GÜLSÜN BAĞCI

MOLECULAR BIOLOGY AND GENETICS

MASTER DISSERTATION

Advisors

Prof. Dr. SAFİYE NEŞE ATABEY
Asst. Prof. HANİ ALOTAİBİ

(This Project is supported by TÜBİTAK in the context of 1003 project with #115E056)

Thesis Code: DEU.İBG.MSc-2016850007



T.C.
DOKUZ EYLÜL ÜNİVERSİTESİ

İZMİR ULUSLARARASI BİYOTIP VE GENOM ENSTİTÜSÜ



YÜKSEK LİSANS TEZ SAVUNMA SINAVI TUTANAĞI

Dokuz Eylül Üniversitesi İzmir Uluslararası Biyotıp ve Genom Enstitüsü Genom Bilimleri ve Moleküler Biyoteknoloji Anabilim Dalı Yüksek Lisans Programı 2016850007 numaralı öğrencisi Gülsün BAĞCI, “THE ROLE OF C-MET ACTIVATION ON THE ORGAN SPECIFIC EXTRAVASATION IN HCC CELLS” konulu Yüksek Lisans tezini 26.07.2019 tarihinde yapılan savunma sınavı sonucunda başarılı olmuştur.

BAŞKAN
Dr. Öğr. Üyesi Hani ALOTAİBİ

Dokuz Eylül Üniversitesi
İzmir Uluslararası Biyotıp ve Genom Enstitüsü
Biyotıp ve Sağlık Teknolojileri Anabilim Dalı

ÜYE

Prof. Dr. Neşe ATABEY
İzmir Biyotıp ve Genom Merkezi

ÜYE

Doç. Dr. Güneş ÖZHAN BAYKAN
Dokuz Eylül Üniversitesi İzmir
Uluslararası Biyotıp ve Genom Enstitüsü
Biyotıp ve Sağlık Teknolojileri Anabilim
Dalı

ÜYE

Doç. Dr. Şerif ŞENTÜRK
Dokuz Eylül Üniversitesi İzmir
Uluslararası Biyotıp ve Genom Enstitüsü
Genom Bilimleri ve Moleküler
Biyoteknoloji Anabilim Dalı

ÜYE

Dr. Öğr. Üyesi Ayşe Banu DEMİR
İzmir Ekonomi Üniversitesi Tıp Fakültesi
Temel Tıp Bilimleri Tıbbi Biyoloji
Bölümü

TABLE OF CONTENTS

LIST OF TABLES	iv
LIST OF FIGURES	v
ABBREVIATIONS	ix
ABSTRACT	1
ÖZET	2
1. GENERAL INFORMATION	3
1.1 Tumor Metastasis	3
1.1.1 Migration and invasion of cancer cells.....	3
1.1.2 Intravasation into the Blood Stream or Lymph Node	5
1.1.3 Survival and Transition in the Circulation or Lymphatics	6
1.1.4 Arrest at Target Organs	7
1.1.5 Extravasation	7
1.1.6 Micrometastasis Formation	9
1.1.7 Metastatic Colonization.....	9
1.2 Hepatocellular Carcinoma (HCC)	9
1.3 Intrahepatic and Extrahepatic Metastasis	11
1.4 Cellular Signaling Pathways during Hepatocarcinogenesis	11
1.4.1 WNT/ β -catenin pathway	11
1.4.2 PI3K/AKT/mTOR signaling pathway.....	12
1.4.3 The ERK/MAPK pathway	12
1.4.4 HGF/c-Met Signaling Pathway	12
1.5 Metastatic Models.....	15
1.5.1 Non-animal models	15
1.5.2 Animal Models	15
1.6 Microfluidic Approaches for Mimicking Tumor Microenvironment and Metastasis in vitro	16
1.6.1 Lab-on-a-chip (LOC)	16
2. MATERIALS AND METHODS	19
2.1 Type of Study	19
2.2 Time and Location of Study	19
2.3 Population of Study	19
2.4 Cell Culture and Splitting	19

2.4.1	Culturing HCC Cell Lines	19
2.4.2	Culturing THLE-2 Cell Lines	19
2.4.3	Culturing BEAS-2B Cell Lines	20
2.4.4	Culturing HS-27A Cell Lines	20
2.4.5	Culturing Human umbilical vein endothelial cell (HUVEC) Cell Lines	21
2.4.6	Cell Counting	21
2.4.7	Thawing cells and Freezing the cells	22
2.4.8	Freezing Cells	22
2.5	Fluidic Shear Stress Treatment	22
2.6	Lab-on-a-chip (LOC)	23
2.6.1	Coating of LOCs	23
2.6.2	Loading of Homing Cells and HUVEC Cells	24
2.6.3	Loading of SNU-449 Azurite Monoclonal Cells	25
2.6.4	Loading of SNU-398 CMV GFP (MOCK) and SNU-398 MET GFP Overexpressed Cells	26
2.7	Protein Isolation	27
2.7.1	BCA (Bicinchoninic Acid) Protein Assay	27
2.7.2	SDS-PAGE (Polyacrylamide gel electrophoresis)	27
2.8	MATERIALS	30
2.8.1	Preparation of Solution	30
3.	RESULTS	33
3.1	Homing Cells were transduced with plasmids containing mCherry tagged fluorescent protein with lentivirus	33
3.2	HUVEC (Human Umbilical Vein Endothelial Cells) cells as representing endothelial barrier stained with CellTracker™ Green CMFDA Dye	34
3.3	SNU-449 cells were transduced with plasmid containing Azurite tagged fluorescent protein with lentivirus	34
3.4	Loading of Homing cells to homing channel, HUVEC cells and SNU-449 Azurite monoclonal cells to flow channels on the Extravasation Lab-on-a-chip	35
3.5	Extravasation of Static SNU-449 Azurite monoclonal cells which had constitutively active c-Met RTK to THLE-2, BEAS-2B and HS-27A homing cells	38
3.6	Inhibition c-Met RTK via SU11274 affected on extravasation frequency of SNU-449 Azurite monoclonal cells to THLE-2, BEAS-2B and HS-27A homing cells on the LOC	40
3.7	Inhibition of activate c-Met RTK via SU12274 decreased the extravasation of SNU-449 Azurite monoclonal cells to THLE-2, BEAS-2B and HS-27A homing cells on the LOC.	41
3.8	Extravasation of SNU-449 Azurite monoclonal cells which were exposed to 0.5 dyn/cm ² Fluid Shear Stress for 4 hours to THLE-2, BEAS-2B and HS-27A homing cells ..	42

3.9	Inhibition c-Met RTK via SU11274 affected on extravasation frequency of SNU-449 Azurite monoclonal cells exposed to 0.5 dyn/cm ² FSS for 4 hours to THLE-2, BEAS-2B and HS-27A homing cells on the LOC.....	44
3.10	Determination of Organ Specific Extravasation of SNU-398 c-Met Overexpressed Cells (SNU-398-MET-GFP).....	46
4.	DISCUSSION	48
5.	CONCLUSION.....	53
6.	PERSPECTIVES.....	54
7.	REFERENCES	55
8.	APPENDIX	59
9.	CURRICULUM VITAE (CV).....	60



LIST OF TABLES

Table 2.1 Lists of Equipment used..... 31

Table 3.1 The extravasation percent of SNU-449 cells treated with SU11274 and control group at static condition. 42

Table 3.2 The extravasation percentage of SNU-449 cells treated with SU11274 which exposed to 0.5 dyn/cm² for 4 hours and control group. 45



LIST OF FIGURES

Figure 1.1 Cell Migration. Formation of Src-FAK complex promotes phosphorylation of FAK (1) and p130CAS (2). After c-Crk binds to p130CAS results in activation of Rac and Cdc42 by displacement of DOCK1 (3). Activated Rac activates Arp2/3 via N-WASP/WAVE. Binding of F-actin and Arp2/3 provides the movement of lamellipodia at the front edge (4). Activated JNK by Src causes secretion of MMPs which degrade the ECM at the rear edge (5) and calpain degrades the interaction between Fak and integrins (6)(Playford & Schaller, 2004).....	5
Figure 1.2 Extravasation of tumor cells a) After intravasation of tumor cells, they are covered by platelets which are activated by tumor cells. b) secretion of cytokines by tumor cells, platelets and NK cells activates the endothelium then it promotes recruitment of monocytes. c) TGF- β secreted by platelets activates epithelial-to-mesenchymal transition (EMT) of tumor cells via activation of TGF- β /Smad and NF- κ B (Labelle & Hynes, 2012).....	8
Figure 1.3 Steps of Tumor Metastasis (Valastyan & Weinberg, 2011).....	9
Figure 1.4 Initiation and progression of HCC (Singh, Kumar, & Pandey, 2018).....	10
Figure 1.5 The structure Hepatocyte Growth Factor (HGF). Pro-HGF is the inactive form of HGF which is composed of two subunits as alpha-chain (heavy chain) and beta-chain (light chain) subunits and these subunits are held together via a short spacer part. The conversion of pro-HGF to HGF is performed by serine proteases as matriptase, hepsin and HGF activator (HGFA) enzymes at Arg 494-Val 495 cleavage site (NAKAMURA & MIZUNO, 2010).	13
Figure 1.6 Canonical and Non-canonical Pathways of c-Met. Binding of HGF to c-Met induces homodimerization of c-Met receptor then leads to autophosphorylation of Y1234 and Y1235 tyrosine residues and binding of effector proteins results in activation of canonical pathway. In the non-canonical pathway, c-Met monomer dimerizes with different receptor monomer leading to activation of different cellular events based on dimerized receptor (García-Vilas & Medina, 2018).....	14
Figure 1.7 Microfluidic Systems. Development in the 3D cell culture system involves mechanical changes in cells for metastatic studies (Malandrino, Kamm, & Moeendarbary, 2018).....	16
Figure 2.1 Cell counting. The cells on the five squares/areas on Neubauer hemocytometer were counted twice.....	21
Figure 2.2 Fluidic Shear Stress Treatment. Watson Marlow 205U peristaltic pump, Marprene Tube Elements for 2.79 bore Watson Marlow tubing and bubble traps were used.	23

Figure 2.3 Vacuum Desiccator	24
Figure 2.4 Western blot result of c-Met expression and activation of SNU-449 and SNU-398 cells (Unpublished data, Atabey N.).	25
Figure 2.5 Experimental Design for loading of SNU-449 Azurite cells to Lab-on-a-chip	26
Figure 2.6 Organization of sandwich system for transfer of proteins from gel to PVDF membrane.	29
Figure 3.1 The top images were fluorescent images of THLE-2 mCherry polyclonal cells as representing liver epithelial cells, BEAS-2B mCherry polyclonal cells as representing lung epithelial cells HS-27A mCherry polyclonal cells as representing bone marrow/stroma cells respectively and the bottom images were DIC images of them respectively by using Olympus IX71 Fluorescence microscope under 10X objective via red filter and DIC.	33
Figure 3.2 HUVEC cells were stained with 5 μ M Green Cell Tracker respectively and the bottom images were DIC images of them respectively by using Olympus IX71 Fluorescence microscope under 10X objective via green filter and DIC.....	34
Figure 3.3 Fluorescent and DIC images of SNU-449 Azurite monoclonal cells respectively by using Olympus IX71 Fluorescence microscope under 20X objective via blue filter and DIC.	35
Figure 3.4 Tile scale image of homing channel of extravasation LOC with of THLE-2 (600.000 cells/100 μ l) , BEAS-2B (600.000 cells/100 μ l) and HS-27A (300.000 cells/100 μ l) mCherry polyclone homing cells in matrigel respectively. (The tile scan image was taken under Zeiss LSM 880, Axio Observer microscope at Izmir Biomedicine and Genome Center by using 594 nm laser and 594 nm filter under 5X objective. The image was analysed via ZEN Blue programme).	35
Figure 3.5 a) The first day the tile scan image and post image of HUVEC cells b) The <i>z-stack</i> images HUVEC cells stained with Green Celltracker in the circulation channel of extravasation LOC was coated the endothelial barrier through 7 days and the images of 1st, 3rd, 5th and 7th day of HUVEC coating. The <i>z-stack</i> image was taken under Zeiss LSM 880, Axio Observer microscope at Izmir Biomedicine and Genome Center by using 488 nm laser and 488 nm filter under 10X objective. The image was analysed via ZEN Blue programme.	36
Figure 3.6 The first day image of intact extravasation LOC.....	37
Figure 3.7 The post image of extravasation (+) and extravasation (-) for SNU-449 Azurite monoclonal cells. Extravasation of SNU-449 Azurite monoclonal cells to HS-27A (6th day for incubation) cells and the extravasation (-) image for SNU-449 cells to BEAS-2B homing cells (3rd day for incubation) for static condition. White arrow shows SNU-449 Azurite cells.	

(The post image was taken under Zeiss LSM 880, Axio Observer microscope at Izmir Biomedicine and Genome Center by using 594 nm, 488 nm and 405 nm laser and 594 nm filter, 488 nm filter and DAPI filter, under 5X objective. The image was analysed via ZEN Blue programme)..... 38

Figure 3.8 7.days images of extravasated SNU-449 Azurite monoclonal cells to THLE-2, BEAS-2B and HS-27A homing cells on the LOC respectively for static condition. White arrow shows SNU-449 Azurite cells. (The 2D images were taken under Zeiss LSM 880, Axio Observer microscope at Izmir Biomedicine and Genome Center by using 594 nm, 488 nm, 405 nm laser and 594 nm filter, 488 nm and DAPI filter under 5X objective. The image was analysed via ZEN Blue programme). 39

Figure 3.9 Extravasation (+) and extravasation (-) post numbers for SNU-449 cells for static condition were determined in accordance with homing organs as THLE-2, BEAS-2B and HS-27A cells after seven day incubation (left) and the extravasation percent of each homing organ was determined by ratio of extravasated post to extravasated negatif post in itself. 39

Figure 3.10 The pie chart for extravasation ratio of SNU-449 cells to THLE-2, HS-27A and BEAS-2B cells at static condition. 40

Figure 3.11 7.days images of SNU-449 Azurite monoclonal cells were treated with SU11274 to THLE-2, BEAS-2B and HS-27A homing cells on the LOC respectively for static condition. The arrow shows their location in the circulation channel and they they were not passed through the HUVEC endothelial barrier. White arrow shows SNU-449 Azurite cells. (The 2D images were taken under Zeiss LSM 880, Axio Observer microscope at Izmir Biomedicine and Genome Center by using 594 nm, 488 nm, 405 nm laser and 594 nm filter, 488 nm and DAPI filter under 5X objective. The image was analysed via ZEN Blue programme). 41

Figure 3.12 Treatment of SU11274 caused a decrease in the extravasation rate of SNU-449 cells as 70.12% in total. Inhibition of activation of c-Met RTK via SU12274 decreased the extravasation rate of SNU-449 Azurite monoclonal cells to THLE-2 cells as 76.93% and to HS-27A cells as 85.79% and to BEAS-2B cells as 38.1% at static condition. **** p<0.0001, ***p<0.001, **p<0.01, *p<0.05, Statical analyses were by Chi-square test of prospective data. 42

Figure 3.13 The extravasation +/- posts was determined for each homing cells for SNU-449 cells which were exposed to 0.5 dyn/cm² FSS for 4 hours based on the data obtained at 7th day after incubation and the extravasation percent of each homing organ was determined by ratio of extravasated positive post to extravasated negatif post in itself. **** p<0.0001,

***p<0.001, **p<0.01, *p<0.05, Statical analyses were by Chi-square test of prospective data. 43

Figure 3.14 The pie chart for extravasation ratio of SNU-449 cells exposed to 0.5 dyn/cm² for 4 hours to THLE-2, HS-27A and BEAS-2B cells..... 44

Figure 3.15 Treatment of SU11274 caused a decrease in the extravasation rate of SNU-449 cells as 49.26% in total. Inhibition of activation of c-Met RTK via SU12274 decreased the extravasation rate of SNU-449 Azurite monoclonal cells which exposed to 0.5 dyn/cm² FSS for 4 hours to THLE-2 cells as 86.24%, and to HS-27A cells as 42.43% and to BEAS-2B cells as 22.84%. **** p<0.0001, ***p<0.001, **p<0.01, *p<0.05, Statical analyses were by Chi-square test of prospective data. 44

Figure 3.16 The comparison of extravasation change of SNU-449 cells at static and FSS exposed condition. The extravasation rate of SNU-449 cells were decreased 35.72% for THLE-2 cells when they were exposed to FSS and the extravasation rate of HS-27A and BEAS-2B cells was increased as 40% and 17% respectively. 45

Figure 3.17 The extravasation+/- post number, % extravasation rate and the organ specific extravasation of SNU-398-MET-GFP cells by pie chart at static condition..... 46

Figure 3.18 The extravasation+/- post number, % extravasation rate and the organ specific extravasation of SNU-398-CMV-GFP cells by pie chart at static condition. 47

Figure 3.19 The presence or absence of c-Met RTK affected the extravasation of SNU-398 cells to THLE-2 liver epithelial cells significantly, **** p<0.0001, ***p<0.001, **p<0.01, *p<0.05, Statical analyses were by Chi-square test of prospective data..... 47

ABBREVIATIONS

HCC: Hepatocellular Carcinoma

HGF : Hepatocyte Growth Factor

HGFA: Hepatocyte Growth Factor Activator

LOC : Lab-on-a-Chip

RTK : Receptor Tyrosine Kinase

RT-qPCR: Reverse-transcriptase quantitative polymerase chain reaction

SF: Scattering Factor

ECM: Extracellular Matrix

BM: Basal Membrane

VEGF: Vascular Endothelial Growth Factor

CDK: Cyclin-dependent kinase

MMP: Matrix Metalloproteinase

FAK: Focal Adhesion Kinase

uPA/uPAR: Urokinase-type plasminogen activator system

VCAM-1: Vascular Cell Adhesion Molecule 1

2D: Two-Dimensional

3D: Three-Dimensional

GRB2: Growth factor receptor bound protein 2

PDMS: Polydimethylsiloxane

HUVEC: Human Umbilical Vein Endothelial Cell

TEM: Transendothelial Migration

PD-L1: Programmed Death Ligand 1

MAPK: Mitogen-activated protein kinase

CTCs: Circulating Tumor Cells

DTCs: Disseminated Tumor Cells

CoC: Cancer-on-a-Chip

PVDF: Polyvinylidene Fluoride

Angpt2: Angiopoietin2

CXCR4: Chemokine Receptor 4

GAPs: GTPase-activating proteins

DMSO : Dimethyl sulfoxide

PECAM-1: Platelet and Endothelial Cell Adhesion Molecule 1

JNK: c-Jun N-terminal kinase

L1-CAM: L1 cell adhesion molecule

CAFs : Carcinoma-associated fibroblast



ACKNOWLEDGEMENTS

I would first like to thank my advisor, Prof. Dr. Neşe Atabey at Izmir Biomedicine and Genome Center for giving me this opportunity to study with her and to achieve this study. I am very grateful to her for her support and great guiding all the time. The door of her office was open all the time whenever I had a question or problem and she always guided with her great experience and smiling. Moreover, I would like to thank Asst. Prof. Hani Alotaibi for his support all the time.

I would like to thank to my lab friends for their endless support, their friendships and spending good time together. Dehan Çömez, also my classmate, always provided full support whenever I needed. I really appreciate everything he did and special thanks for his contributions. He was a wonderful friend and scientist. Hande Topel had a high problem solving ability and whenever I had a trouble she always found a way to overcome and special thanks for her friendship and great contributions. Ezgi Bağırşakçı saved my life many times with her retentive memory and special thanks for her friendship and contributions. I would like to thank to Yeliz Yılmaz, Ayşim Güneş, Peyda Korhan, Yasemin Öztemur Islakoğlu and Sanem Tercan Avcı for their unflagging support, sharing their experiences and spending quality time together.

I would like to thank to members of Optical Imaging Core Facility at Izmir Biomedicine and Genome Center Dr. Melek Üçüncü and Didem Çitay for their patiently helping and their politeness.

I would like to thank to Aybike Erdoğan, Başak Gündüz, Deniz Kurşun, Burcu Akman, Canan Çeliker, Kübra Nur Kaplan, Olcay Burçin Akbulud and Kadriye Güven for their friendships and always being supportive during this difficult period.

I would like to thank to Assoc. Prof. Dr. Devrim Pesen Okvur and her group at Izmir Institute of Technology for providing Lab-on-a-chip devices.

I would like to thank to my family for supporting me all the time and I am grateful to them for their endless confidence.

“one small step for man one giant leap for mankind”

THE ROLE OF c-MET ACTIVATION ON THE ORGAN SPECIFIC EXTRAVASATION IN HEPATOCELLULAR CARCINOMA CELLS

Gülsün Bağcı, Dokuz Eylül University Izmir International Biomedicine and Genome Institute, gulsun.bagci@msfr.ibg.edu.tr

ABSTRACT

HCC is the fifth most common cancer worldwide and the third cause of cancer deaths. Due to difficulties in diagnosis, many patients are diagnosed at late stages. HCC is associated with high mortality rate due to high recurrence, metastasis risk after surgical resection. c-Met signaling pathway mediates embryogenesis and organ regeneration, its aberrant activation can promote invasion, motility, proliferation, angiogenesis and evading apoptosis in several cancers including HCC. Recent data suggest that activation of c-Met signaling might be an important factor in the regulation of tumor metastasis. However, role of c-Met signaling in the organ specific extravasation is not defined. Lab-on-a-chip is integrated 3D cell culturing to study for tumor-microenvironment interactions, drug screening, studying metastatic patterns of cancer cells to distant organs. In this study, a Lab-on-chip device was used to mimic the extravasation capacities of SNU-449, SNU-398, SNU-398-Met HCC cells to investigate role of c-Met on the organ specific extravasation. Homing cells were THLE-2, BEAS-2B and HS-27A to represent liver epithelial, lung epithelial and bone marrow/stroma cells respectively. HUVEC cells were used to mimic endothelial barrier. As a result, activation of c-Met signaling is significantly increased organ specific extravasation of HCC cells and c-Met inhibitor SU11274 decreased extravasation rate of HCC cells approximately 70% in total. Our data support that c-Met signaling could play role in organ specific extravasation especially in intrahepatic metastasis and bone metastasis and SU11274 could be used as anti-cancer drug to prevent metastasis especially to prevent HCC and can be used for therapeutic purposes.

Keywords: HCC, c-Met, metastasis, extravasation

HEPATOSELÜLER KARSİNOMA HÜCRELERİNDE ORGAN SPESİFİK EKSTRAVAZASYONDA C-MET YOLAĞININ ROLÜNÜN İNCELENMESİ

Gülsün Bağcı, Dokuz Eylül Üniversitesi, İzmir Uluslararası Biyotıp ve Genom Enstitüsü,
gulsun.bagci@msfr.ibg.edu.tr

ÖZET

HCC dünya genelinde en sık görülen beşinci kanser türü iken kanser nedeniyle olan ölümlerin üçüncü sebebidir. HCC tanısındaki zorluk nedeniyle, bir çok hastaya ancak ileri evrede tanı konulabilmektedir. HCC’de kansere bağlı ölümlerin en sık sebebi yüksek nüks ve metastazdır. Normal gelişim ve organ rejenerasyonu, yara iyilişmesi gibi süreçlerde rol oynayan HGF/c-Met yolağındaki bozukluklar, HCC de dahil birçok kanser türünde invazyon, motilite, anjiyogenez ve apoptozdan kaçışta önemli rol oynamaktadır. Son yıllarda c-Met aktivasyonunun organ spesifik metastaz ile ilişkili olabileceğini destekleyen bazı veriler elde edilmiştir. Ancak, HCC hücrelerinin ekstrasvazasyonu ve organ terchinde HGF/c-Met yolağının rolü henüz tanımlanmamıştır. LOC sistemleri hücre kültürü, hücre örneklemesini, akışkan kontrolünü tek bir cihazda toplayan bir sistemler olup, in vivo koşulları taklit eden üç boyutlu (3D) ko-kültür koşullarında tümör hücrelerinin biyolojik davranışlarını, hücre içi sinyal yollarını incelemede, çoklu ilaç direnci ve ilaç taraması gibi uygulamalarda kullanılmasına olanak sağlamaktadır. Bu tez çalışması kapsamında SNU-449, SNU-398, SNU-398-Met HCC hücrelerinin organ spesifik ekstrasvazasyonda c-Met yolağının rolü yonga-üstü-laboratuvar (LOC) cihazı kullanılarak incelendi. Normal hücreleri olarak THLE-2 karaciğer epitelyal hücreleri, HS-27A kemik iliği stroma hücrelerini ve BEAS-2B akciğer epitelyal hücreleri kullanıldı. HUVEC hücreleri, damar yapısını taklit etmek için kullanıldı. Sonuç olarak, c-Met sinyal yolağının aktivasyonu HCC hücrelerinin organ spesifik ekstrasvazasyonunu anlamlı olarak arttırırken, c-Met inhibitörü SU11274 kullanımı HCC hücrelerinin ekstrasvazasyonunu toplamda yaklaşık olarak %70 oranında azaltmıştır. Elde ettiğimiz veriler c-Met sinyal yolağının özellikle intrahepatik ve kemik metastazında organ spesifik ekstrasvazasyonda rol oynayabileceği ve c-Met inhibitörü SU11274 metastazı engellemek için kansere karşı ilaç olarak özellikle HCC’yi engellemek için ve terapatik hedefler için kullanılabileceğini gösterdi.

Anahtar Kelimeler: HCC,c-Met, metastaz, ekstrasvazasyon

1. GENERAL INFORMATION

In 1889, “seed and soil” hypothesis, “*When a plant goes to seed, its seeds are carried in all directions; but they can only live and grow if they fall on congenial soil*” was proposed by Stephan Paget (Zelinsky & Newman, 1974). He studied on above 900 autopsied patients who had different types of primary tumors. According to this hypothesis, metastasis is not a random process and there is a certain affinity between cancer cells (seed) and microenvironment of specific organs (soil). This hypothesis is widely accepted, and it still provides significant achievements in cancer research until today. The modern view of the “seed to soil” hypothesis have three principles: (i) tumors are heterogenous and tumor cells have different invasion and metastasis capacities, (ii) metastasis is selective for cells which are capable of invasion and extravasation, survival in circulation, and extravasation and homing in a distant organ. (iii) metastasis is dependent on the interaction of tumor microenvironment (Zelinsky & Newman, 1974).

1.1 Tumor Metastasis

Metastatic cancer occurs when tumor cells disseminate from primary tumor and form secondary tumors at another side of body. Metastasis is the sequential steps of dissemination of cancer cells from primary tumor to colonize secondary organs, also called as invasion-metastasis cascade. The formation of metastases is ineffective naturally, however, when the metastasis process is accomplished, cancer becomes untreatable. That's why, metastasis leads to nearly 90% of all cancer-associated deaths (Valastyan & Weinberg, 2011). The process of tumor metastasis is consists of seven sequential steps as (Fig.1.3):

- 1) local invasion, dissemination of cancer cells from primary tumor,
- 2) intravasation into the blood stream or lymph nodes,
- 3) survival in the circulation,
- 4) arrest in the distant organs,
- 5) extravasation,
- 6) micrometastasis formation,
- 7) metastatic colonization

1.1.1 Migration and invasion of cancer cells

The initial step of metastasis is invasion which is alteration in the attachment of tumor cells, degradation of adjacent tissue and migration of tumor cells. Integrins play role in attachment of tumor cells to Extracellular Matrix (ECM). Transmembrane proteins as cadherins mediate cell-cell adhesion via catenins and actin cytoskeleton. Upregulation of N-cadherins' expression and

down regulation of E-cadherins promotes invasion. Binding of integrins and anchorage molecules promote the proteases such as matrix metalloproteinases, plasmin, urokinase plasminogen activator, cathepsins and heparanases to degrade ECM for enhancement of the invasion. Moreover, proteases play role in activation of some surface proteins which are important for tumorigenesis by providing secretion of some growth factors and chemokines. Invasion is a dynamic process which is moving of tumor cells as attachment of cell's leading edge to ECM and disconnection of rear edge of the cell from the ECM. Chemokines also facilitate the invasion of tumor cells by recruitment of macrophages, lymphocytes secreting proteases and inflammatory molecules (Steeg, 2006). Src is a nonreceptor tyrosine kinase which is composed of a N-terminal domain, a SH3, SH2 domain, a C-terminal domain and tyrosine domain. Phosphorylation at tyrosine 416 results in autophosphorylation and phosphorylation at tyrosine 527 residue located at C-terminal domain inhibits catalytic activity of Src. Absence of tyrosine 527 residue located at C-terminal domain leads to constitutive activation of Src which is called as *V-Src*. Integrins are heterodimeric transmembrane proteins composed of α and β subunits. They play role in migration, invasion and cell anchorage (Mierke, 2008)(Mierke, 2008). Assembly of different α as 18 different subunits and β as 8 different subunits provides the formation of different receptors. These different receptors bind to different ligands on the ECM such as collagen, fibronectin, and laminin and other proteins like Vascular Cell Adhesion Molecule 1 (VCAM-1), Platelet And Endothelial Cell Adhesion Molecule 1(PECAM-1) (Mierke, 2008). In addition, the interplay between receptor tyrosine kinases (RTKs) and integrins promotes the FAK-Src complex formation which activates Rac results in MMP secretion and lamellipodia forming. Paxillin and talin promote the binding of Fak and integrins. Binding of p130CAS, CRK and the DOCK180-ELMO complex to Fak activates Rac. The interaction between Fak and N-WASP leads to activating GTPase which activates Arp2/3. Binding of F-actin and Arp2/3 provides the movement of lamellipodia. Binding of p190RhoGEF to Fak activates Rho which provides formation of actin stress fiber. Activation of c-Jun N-terminal kinase (JNK) by Src leads to secretion of MMPs which degrade the ECM at the rear edge. Moreover calpain degrades the interaction between Fak and integrins (Fig.1.1)(Playford & Schaller, 2004).

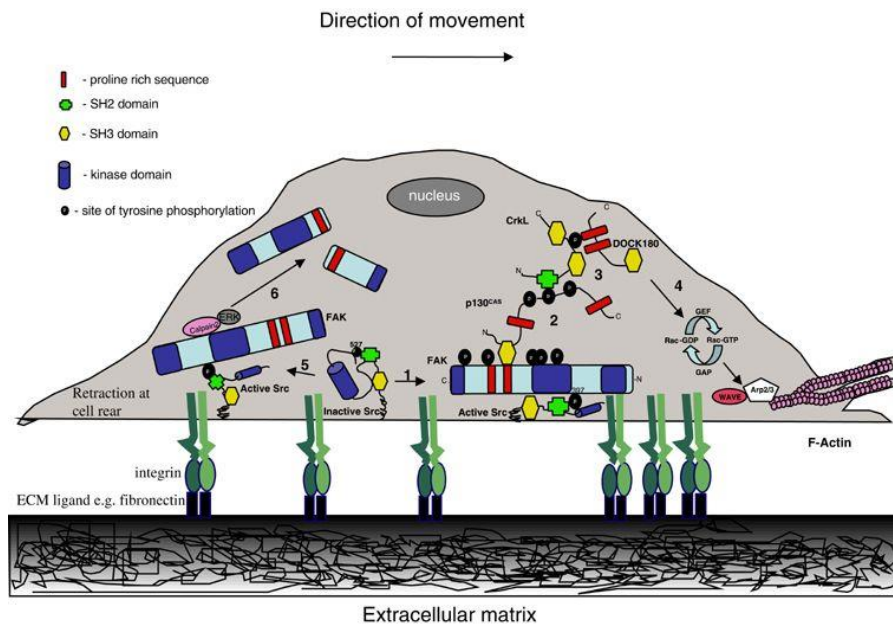


Figure 1.1 Cell Migration. Formation of Src-FAK complex promotes phosphorylation of FAK (1) and p130CAS (2). After c-Crk binds to p130CAS results in activation of Rac and Cdc42 by displacement of DOCK1 (3). Activated Rac activates Arp2/3 via N-WASP/WAVE. Binding of F-actin and Arp2/3 provides the movement of lamellipodia at the front edge (4). Activated JNK by Src causes secretion of MMPs which degrade the ECM at the rear edge (5) and calpain degrades the interaction between Fak and integrins (6)(Playford & Schaller, 2004).

Another signaling pathway promotes invasion is HGF/c-Met pathway. Binding of HGF to c-Met causes activation of c-Met following binding of GAB1 adaptor protein to active c-Met. Activated PTP Shp2 activates Rac results in increasing invasion (Steeg, 2006). There are two mechanisms as epithelial-mesenchymal transition EMT-mediated and non-EMT-mediated invasion of cancer cells from primary tumor. After recruitment of stromal cells by cancer cells in the inflammatory microenvironment, stromal cells secrete many cytokines and activate EMT-induced transcription factors such as SNAIL, TWIST, and ZEB which downregulate E-cadherin expression. Moreover, hypoxia can activate EMT. EMT is a process starting with losing of cell-cell contacts such as tight junctions, adherens junctions, desmosomes and gap junctions and depolarization of epithelial cells. Downregulation of epithelial gene expression and upregulation of mesenchymal gene expression occurs. After organisation of epithelial actin, cells form lamellipodia, filopodia and invadopodia and express matrix metalloproteinases (MMP-1, -2, and -9) and activation of the proteolytic urokinase-type plasminogen activator system (uPA/uPAR) so as to break basal membrane (BM) and extracellular matrix (ECM) proteins (Pachmayr, Treese, & Stein, 2017).

1.1.2 Intravasation into the Blood Stream or Lymph Node

There are three mechanisms for tumor cells during intravasation as transmigration of tumor cells over the cell body's cytoplasm, stimulation of apoptosis by tumor cells on the endothelial

cells for migration by means of this puncture and transmigration of tumor cells via endothelial-endothelial cell contacts (Mierke, 2008). Invasive cancer cells penetrate into the blood vessels via passive infiltration occurring due to leaky vasculature to provide nutrients and oxygen for tumor growth and transendothelial migration. Cancer cells can migrate as single cell or in cluster. Single cell undergoes EMT and cells in cluster possess cell-cell contacts and they are composed of different cell types such as cancer cells and cancer-associated fibroblasts (CAFs) facilitating survival of cancer cells. In non-EMT-mediated invasion cancer cells accidentally enter into circulation due to tumor growth or external forces. Tumor cells promote the formation of new blood vessels which is known as neoangiogenesis. The vessels generated via neoangiogenesis are leaky and they have incomplete pericyte encapsulation. Secretion of vascular endothelial growth factor (VEGF) promotes formation of new vessels. Therefore, this facilitates the intravasation of cancer cells. Secretion of MMP-1, -2 and -9 and activation of uPA/uPAR lead to intravasation of cancer cells into vasculature or lymphatic vessel (Pachmayr et al., 2017). The interaction between L1 cell adhesion molecule (L1-CAM) and PECAM-1 expressed on the endothelial cells and $\alpha\beta3$ integrin on the tumor cells facilitate the transmigration of tumor cells. Moreover, L1-CAM and P-selectin expressed on the endothelial cells interact with CD24 expressed on the tumor cells results in enhance of the cancer cell migration (Mierke, 2008).

1.1.3 Survival and Transition in the Circulation or Lymphatics

After cancer cells intravasation into circulation or lymphatics, majority of them are eliminated by immune cells, fluid shear stress (FSS) and oxidative stress in the blood environment and absence of ECM attachment in other words undergoing anoikis. Anoikis is a type of apoptosis of normal cells due to lack of ECM anchorage. Cancer cells control the anoikis via regulating the pentose phosphate pathway and glucose uptake. The cancer cells escaped from immune cells and resistant to circulatory conditions are able to finalize metastasis. Circulating tumor cells (CTCs) survive by activating Akt signaling pathway and regulate their integrin expression. CTCs escape from immune cells by upregulating some surface proteins as CD47, the programmed death ligand 1 (PD-L1) and vascular cell adhesion molecule 1 (VCAM-1). PD-L1 is “don't find me” signal to adaptive immune system and CD47 is “don't eat me” signal to innate immune system and adaptive immune system. Only 0.02% of CTCs is able to form metastases even although millions of CTCs are circulated every day (Huang et al., 2018). Cancer cells are resistant to anoikis due to expression of anti-apoptotic BCL2 proteins induced by integrin signaling pathway. Cancer cells take advantage of anoikis due to mutations in the RAS and

PTEN which is tumor suppressor and activation in the Src kinase. p53 mutations are also common which provide cancer cells to elude apoptosis. Anoikis induces apoptosis via extrinsic pathway of apoptosis activated through Fas death receptors results in caspase-8 activation. However, some cancer cells such as in lung and colorectal cancer express decoy receptors for Fas ligand to block the apoptosis. Presence of p16 which is inhibitor of cyclin-dependent kinase (CDK) causes cell cycle arrest and increases the expression of $\alpha 5\beta 1$ integrin. Absence of p16 leads to resistant to anoikis and down regulation of $\alpha 5\beta 1$ integrin which could perceive lack of ECM anchorage (Guo & Giancotti, 2004).

1.1.4 Arrest at Target Organs

It is widely accepted by clinicians that circulating tumor cells (CTCs) are arrested at the specific organs. The arrest of cancer cells at the target tissue whether is originated from tissue tropism which is a certain affinity between cancer cells and target tissue such as ligand-receptor binding between CTCs and capillary endothelial cells or is derived from size of vasculatures that is unclear. Due to diameter of blood vessels, some CTCs are trapped in the microvessels and form emboli. This physical obstacle binds to endothelium of target organ's vessels. For instance, majority of colorectal cancer cells is trapped in the portal vein in the liver and some CTCs are trapped fast (Gupta & Massagué, 2006). However, some of them are circulated to distant organs due to their plasticity or by chance. The other hypothesis is organ-specific trapping of CTCs, there is a specific interaction between CTCs and endothelium of target organ's vessel. For instance, due to expression of Metadherin on the breast cancer cells, they are lodged in lung vessels (Brown & Ruoslahti, 2004).

1.1.5 Extravasation

Extravasation is the penetration of CTCs from endothelial barrier and pericytes to homing organs. There is a specific affinity between CTCs and particular organs which is called as organ tropism/tissue tropism. The composition of microenvironment and barrier of each organs are different from each others. Determination of tissue tropism is important for both prediction of target metastatic tissue and targeted drug therapies. For instance, breast cancer cells expressed chemokine receptor 4 (CXCR4) are migrated to the organs which possess high level of the receptor's ligand, CXCL12 as lung, liver, bone marrow, brain. Moreover, primary tumor secretes various proteins for vascular hyperpermeability. This facilitates extravasation of CTCs. Many primary tumors secrete angiopoietin2 (Angpt2), MMP-3, MMP-10, placental growth factor, and VEGF for vascular hyperpermeability in lungs resulting in promoting extravasation of CTCs (Pachmayr et al., 2017).

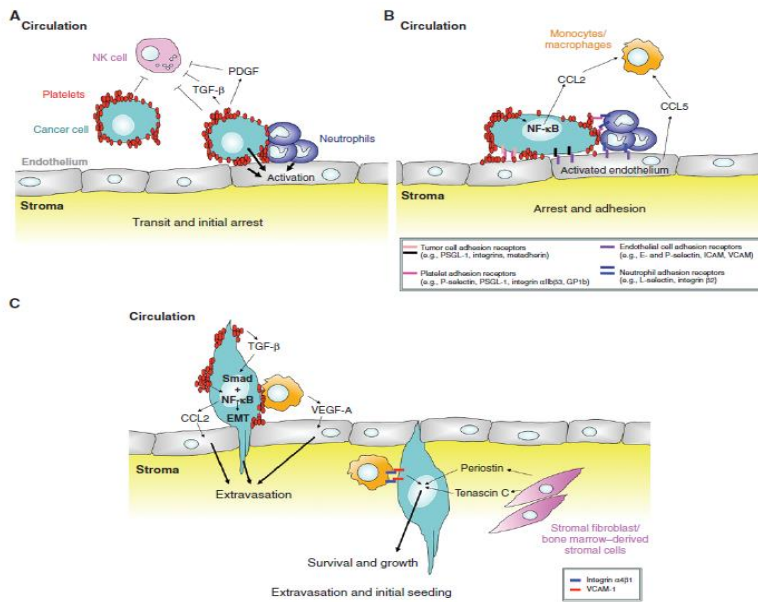


Figure 1.2 Extravasation of tumor cells a) After intravasation of tumor cells, they are covered by platelets which are activated by tumor cells. b) secretion of cytokines by tumor cells, platelets and NK cells activates the endothelium then it promotes recruitment of monocytes. c) TGF- β secreted by platelets activates epithelial-to-mesenchymal transition (EMT) of tumor cells via activation of TGF- β /Smad and NF- κ B (Labelle & Hynes, 2012). After tumor cells enter into circulation, they are immediately covered by platelets. Tissue factor (TF) expressed by tumor cells leads to production of thrombin via plasmatic coagulation process results in activation of platelets and formation of coagulation (Fig.1.2a). Moreover, thrombin enhances transendothelial migration (TEM) by inducing breakdown of adheren junction between endothelial cells to a circular shape of cells. Activation of platelets can be performed via MMP secreted by tumor cells and by neutrophils. Platelets evade tumor cells from immunosurveillance and fluid shear stress. In addition, platelets protect cancer cells from anoikis by activating YAP-1 pathway in ovarian cancer cell lines. Platelets enhanced the metastases in the lungs in contrast to metastases in liver (Schlesinger, 2018). Secretion of interleukin (IL)-1 α , IL-1 β , or TNF- α causes activation of endothelial cells by increasing expression of E-selectin, P-selectin, VCAM-1 and ICAM-1 which are necessary for tumor rolling and adhesion to endothelium. For instance, Kupffer cells secrete TNF- α during metastasis which enhancing the activation of endothelium cells and extravasation of tumor cells. Extravasation usually takes 1 to 3 days. TGF- β secreted by platelets activates epithelial-to-mesenchymal transition (EMT) of tumor cells *in vitro* via activation of TGF- β /Smad and NF- κ B (Fig.1.2c). After activation of endothelium, they produce CCL5 which promotes binding of monocytes to tumor cells and facilitates TEM of tumor cells through endothelium (Fig.1.2b) (Labelle & Hynes, 2012).

1.1.6 Micrometastasis Formation

Colonization is a one rate-limiting step of metastasis. After CTCs are extravasated to distant organs, it is now called disseminated tumor cells (DTCs). DTCs must evade immunosurveillance so as to survive. DTCs cells will form micrometastasis in case of adapted to microenvironment of homing organs. Supportive niches provide them to stay alive and to sustain their tumor initiation capabilities. The cancer cells can stay in dormancy from months to years. After the latent state, they start to form overt metastases. There are two types of latency of tumor as one of them is dormancy of proliferation of DTCs or micrometastasis (Massagué & Obenauf, 2016).

1.1.7 Metastatic Colonization

Decreasing of growth inhibitory molecules or immunosurveillance enable initiation of metastatic colonization. Indeterminable micrometastases are proliferated to form macrometastases which are clinically detectable metastases. Approximately, 50% of patients indicates manifestation of metastases, the rest of them shows tumor dormancy. Based on tumor types, recurrence of tumor varies among different organs. For instance, prostate cancer cells have tendency in recurrence in bone tissue. Manifestated tumors are exposed to targeted therapy which causes therapy-induced secretome from the drug sensitive cells and this leads to growth of drug-resistant cells (Massagué & Obenauf, 2016).

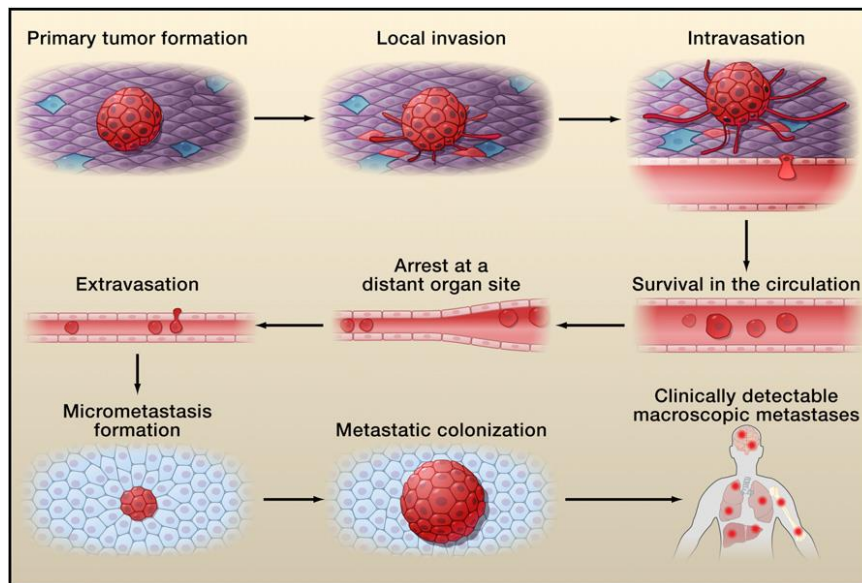


Figure 1.3 Steps of Tumor Metastasis (Valastyan & Weinberg, 2011)

1.2 Hepatocellular Carcinoma (HCC)

HCC (Hepatocellular Carcinoma) is the fifth most common cancer type and the third cause of cancer deaths through the world. The frequency of HCC is higher in males than in females

(Balogh et al., 2016). There are many factors to cause initiation and progression of HCC including infection of hepatitis B (HBV) and C virus (HCV), chronic alcohol consumption, cirrhosis, consuming aflatoxin B1 contaminated food, obesity and type II diabetes (Farazi & DePinho, 2006). 10-25 percent of population who infected with HBV is under the risk of developing HCC (Balogh et al., 2016). HBV has a double-stranded DNA which is capable of integrated into the host genome and causes microdeletions of important genes such as TERT, PDGF β and MAPK1. In addition, The HBx protein promotes the expression of *SRC* tyrosine kinases, Ras, Raf, MAPK, *ERK*, *JNK* which are important genes for cell growth. The direct interaction of HBV with ER causes a raise of the oxidative stress. HCV is a single stranded RNA viruses which are not able to integrate into host genome. The frequency of HCV-infected people develops cirrhosis is greater than the frequency of HBV-infected people. HCV core proteins regulates cell proliferation by reacting with MAPK signaling pathways. Aflatoxin B1 is a mutagen to cause p53 mutation which converts arginine to serine in p53 tumor suppressor gene (Farazi & DePinho, 2006).

HBV, HCV, alcohol consuming or aflatoxin B1 causes injury in liver. MAPK pathway is activated by HBV and HCV. This initiates persistent necrosis and hepatocyte proliferation cycle leading to chronic liver disease results in liver cirrhosis which is formation of abnormal liver nodules surrounding with collagen. During chronic liver disease and liver cirrhosis, telomere becomes shorter. Hyperplastic nodule formation is followed by dysplastic nodule formation and finally HCC develops. HCC can be well differentiated, moderately differentiated or poorly differentiated which is the most malignant form of HCC.(Fig.1.4) (Farazi and DePinho, 2006).

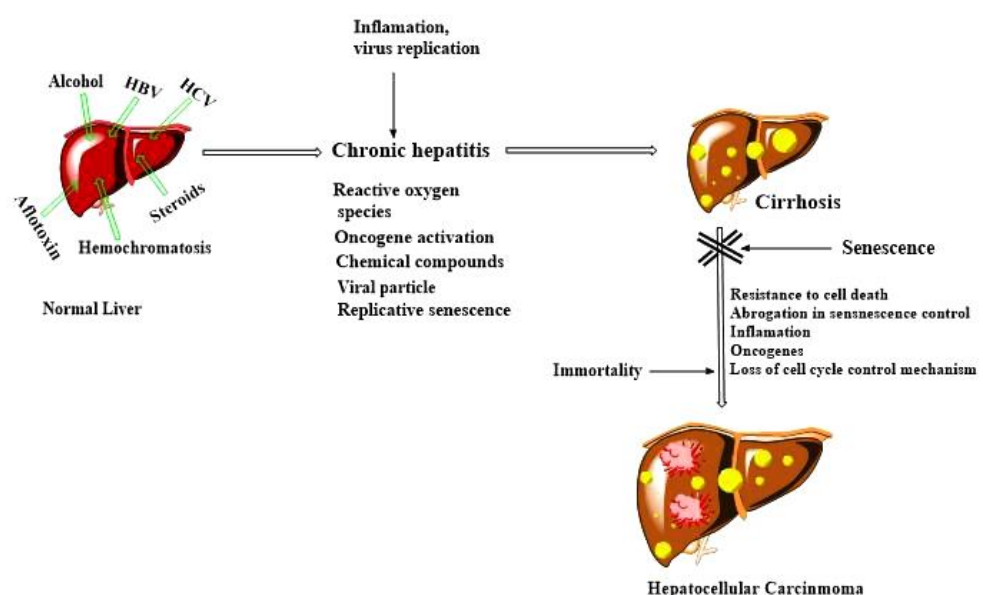


Figure 1.4 Initiation and progression of HCC (Singh, Kumar, & Pandey, 2018)

1.3 Intrahepatic and Extrahepatic Metastasis

Lethality of HCC is derived from diagnosis at advanced stage, recurrence after surgery, high frequency of intrahepatic and extrahepatic metastasis. In contrast to other tumor types, metastasis mainly happens within the liver. 13.5–42% of patients developed HCC is metastasized extrahepatically (Kamimura, 2019). The rate of extrahepatic metastatic sites are lungs (55%), lymph nodes (53%), bone (28%), adrenal glands (11%), peritoneum and/or omentum (11%), and brain (2%) (Becker, Tso, Harris, Malfair, & Chang, 2014). Each organ is different from each other based on their vascular, stromal components, physical accessibility and nutritional source, which affects the infiltration of cancer cells. The circulation design of each organ and structure of their vessels affect the metastasis. For example, the kidney, liver and brain obtain approximately 10-20% of the blood volume, however they all differ in metastasis rate. According to “seed and soil” hypothesis, there is a harmony between the seeds as cancer cells and soils as organs. Different cancers show different organ specific metastasis (Obenauf & Massagué, 2016).

1.4 Cellular Signaling Pathways during Hepatocarcinogenesis

Many signaling pathways activated during hepatocarcinogenesis are due to two important events as i) cirrhosis caused by hepatic injuries originated from alcohol consuming, aflatoxin, infection of viral hepatitis and ii) mutations in oncogene(s) or tumor suppressor gene(s). Some of these signaling pathways are listed as RAF/MEK/ERK pathway, PI3K/AKT/mTOR pathway, WNT/ β -catenin pathway, insulin-like growth factor pathway, HGF/c-MET pathway and angiogenic signaling pathway.

1.4.1 WNT/ β -catenin pathway

Infections of HBV/HCV, cirrhosis caused by alcohol consumption promote activation of WNT/ β -catenin pathway results in increasing of inflammation. Moreover, mutation occur in APC which is tumor suppressor gene or in the protooncogene β -catenin activates WNT/ β -catenin pathway. WNT/ β -catenin pathway regulates motility, proliferation, differentiation, apoptosis. Conditional KO of APC gene in liver of mice caused activation of WNT/ β -catenin pathway results in HCC development. Commonly, activation of WNT/ β -catenin pathway in HCC derived from upregulated frizzled-7 and dephosphorylated β -catenin. Infection of HCV and aflatoxin causes increasing of mutations in β -catenin in HCC patients (Aravalli, Cressman, & Steer, 2013).

1.4.2 *PI3K/AKT/mTOR signaling pathway*

There are two forms of PI 3-Kinase depending on activated by G-proteins or by receptor tyrosine kinases. Activation of these receptors leads to phosphorylation of PIP₂ to produce phosphatidylinositol 3,4,5-trisphosphate (PIP₃) as a second messenger to regulate cell growth and survival. PIP₃ binds to Akt which is serine/threonine kinase from the pleckstrin homology domain. Akt is phosphorylated by mTOR/ricor complex and PDK1 results in releasing of Akt. Activated Akt phosphorylates many target proteins such as mTOR, BAD and some transcription factors like FOXO to regulate survival (Cooper and Hausman, 2007). PI3K/AKT/mTOR signaling pathway is regulated by PTEN as a tumor suppressor phosphatase in normal cells. HBX protein cause a decrease in PTEN expression and mutation or deletion of *PTEN* gene is seen in HCC originated tumors results in constitively or excess activation of PI3K/AKT/mTOR signaling pathway (Whittaker, Marais, & Zhu, 2010).

1.4.3 *The ERK/MAPK pathway*

The ERK/MAPK pathway in other words RAF/MEK/ERK pathway plays role in proliferation, differentiation, angiogenesis and survival (Whittaker et al., 2010). After activation of growth factor receptor, Raf serine-threonine kinase binds to activated Ras-GTP binding protein via GTPase-activating proteins (GAPs). *RAS* is an oncogene which leads to sarcoma in rats and it is known as *rats sarcoma virüs*. Raf serine-threonine kinase has three isoforms as ARAF, BRAF and CRAF. Activated Raf kinase phosphorylates MEK which phosphorylates ERK at threonine and tyrosine residues. Activation of Erk phosphorylates various transcription factors and kinases (Cooper and Hausman, 2007). Mutation in the *RAS* gene and overexpression of growth factor receptors lead to constitutive activation of CRAF. Moreover, HBV infection activates this pathway (Whittaker et al., 2010).

1.4.4 *HGF/c-Met Signaling Pathway*

1.4.4.1 *Hepatocyte Growth Factor (HGF)*

HGF is hepatocyte growth factor which is ligand of c-Met receptor and is also known as scatter factor (SF). HGF is found on the 7q21 chromosome and is composed of 18 exons. Pro-HGF is the inactive form of HGF which is composed of two subunits as 69-kDa alpha-chain (heavy chain) and 34-kDa beta-chain (light chain) subunits and these subunits are held together via a short spacer part. HGF contains alpha-chain located on the N-terminal domain with 4 kringle domains and beta-chain subunits (Organ & Tsao, 2011). HGF is secreted by mesenchymal, stromal cells like fibroblasts, macrophages, renal mesangium and it promotes regeneration in the epithelia cells of liver, kidney, lung, spleen. Some growth factors increase the expression of HGF such as basic fibroblast growth factor, oncostatin M, hypoxia inducible factor 1 α and

nuclear factor κ B (NF- κ B) in contrast to transforming growth factor (TGF) β 1 (NAKAMURA & MIZUNO, 2010). The conversion of pro-HGF to HGF is performed by serine proteases as matriptase, hepsin and HGF activator (HGFA) enzymes (García-Vilas and Medina, 2018). The cleavage site is between alpha-chain and beta-chain as Arg 494-Val 495. In the mature HGF, a crossover chain is formed between Cys 487 in the alpha-chain and Cys 604 in the beta-chain (Fig.1.5). In 1984, Nakamura and Mizuno identified HGF in the serum of 70%-hepatectomized rats which increased the proliferation of hepatocytes in the primary culture. In case of liver injury, HGF production is promoted in the kidney, lung, spleen via endocrine system and is also secreted by Kupffer cells to repair the liver. HGF enhances the tissue repair in many organs in response to injury (NAKAMURA & MIZUNO, 2010). HGF is not only a hepatocyte mitogen but also it plays role in cell differentiation and motility, improving angiogenesis and immune system response (García-Vilas & Medina, 2018).

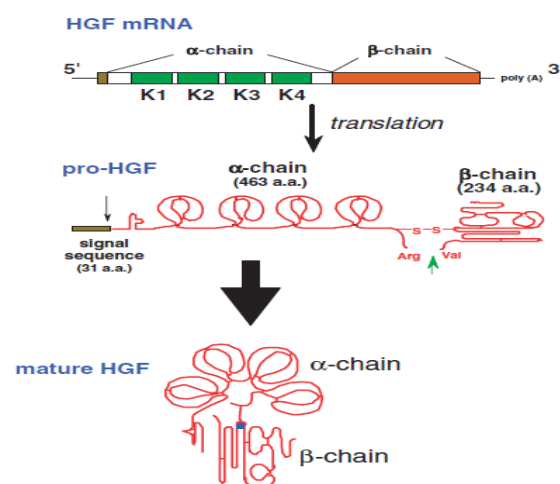


Figure 1.5 The structure Hepatocyte Growth Factor (HGF). Pro-HGF is the inactive form of HGF which is composed of two subunits as alpha-chain (heavy chain) and beta-chain (light chain) subunits and these subunits are held together via a short spacer part. The conversion of pro-HGF to HGF is performed by serine proteases as matriptase, hepsin and HGF activator (HGFA) enzymes at Arg 494-Val 495 cleavage site (NAKAMURA & MIZUNO, 2010).

1.4.4.2 *c-MET* Receptor Tyrosine Kinase

In 1992, Bottaro et al. discovered the c-Met receptor tyrosine kinase (NAKAMURA & MIZUNO, 2010). *MET* is a proto-oncogene stated in other words, the N-methyl-N0-nitrosoguanidine human osteosarcoma transforming gene, which encodes c-MET as a receptor tyrosine kinase (RTK) (Mo & Liu, 2017). The length of *MET* is 125 kb found on the 7q21-q31 chromosome and is composed of 21 exons. The promoter region of c-Met is located on the chromosome 1. c-MET is consist of two subunits as 50-kDa alpha chain and 145-kDa beta-

chain subunits (Mo & Liu, 2017). c-MET is a transmembrane protein containing Sema domain, Plexins, Semaphorins and Integrins (PSI) domain, Immunoglobulin-Plexin-Transcription (IPT) domain, juxtamembrane domain and kinase domain (Organ & Tsao, 2011). N-terminal and C-terminal domain is located on the extracellular and intracellular respectively. Beta subunit contains Y1234, Y1235, Y1349, Y1356 tyrosines in the C-terminal domain which regulate c-Met positively and Y1003 tyrosine regulates c-Met negatively which binds to the ubiquitin ligase c-CBL (Organ & Tsao, 2011). c-Met is commonly expressed on liver cells, fibroblasts, hematopoietic cells, and keratinocytes (Mo & Liu, 2017). c-Met plays role in invasion, motility, proliferation, protecting cells from apoptosis, angiogenesis (García-Vilas & Medina, 2018).

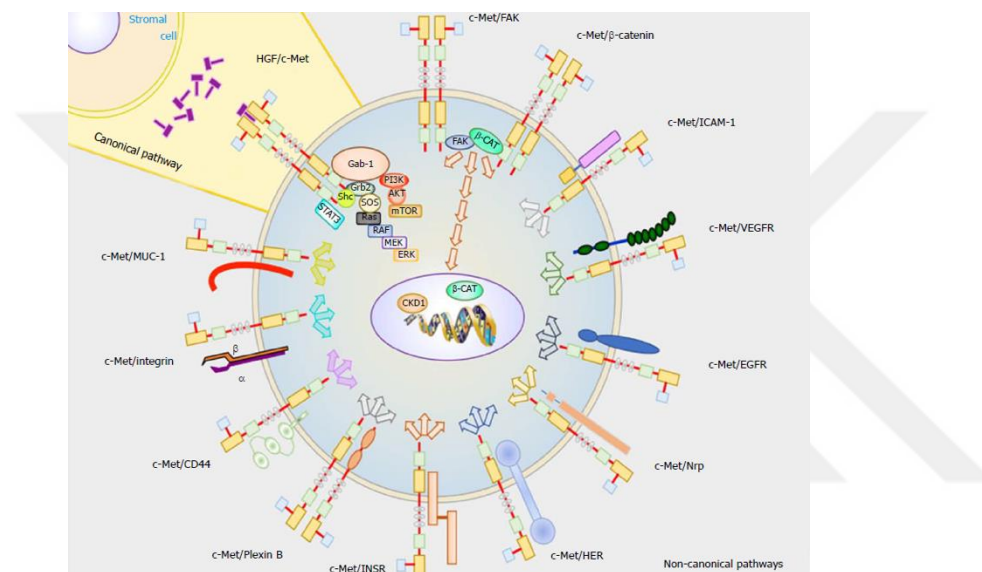


Figure 1.6 Canonical and Non-canonical Pathways of c-Met. Binding of HGF to c-Met induces homodimerization of c-Met receptor then leads to autophosphorylation of Y1234 and Y1235 tyrosine residues and binding of effector proteins results in activation of canonical pathway. In the non-canonical pathway, c-Met monomer dimerizes with different receptor monomer leading to activation of different cellular events based on dimerized receptor (García-Vilas & Medina, 2018).

c-Met can be activated via canonical and non-canonical pathway. Binding of HGF to c-Met induces homodimerization of c-Met receptor then leads to autophosphorylation of Y1234 and Y1235 tyrosine residues. Then Y1349, Y1356 tyrosines are phosphorylated. These tyrosines are docking sites containing SH2 recognition motif for molecules such as Growth factor receptor bound protein 2 (GRB2). Binding of different proteins to activated c-Met tyrosine residues leads to activation invasion, motility, proliferation, survival and so on. This is canonical activation of c-Met receptor. Moreover, the non-canonical pathway, c-Met monomer dimerizes with different receptor monomer in case of *MET* gene amplifications (Fig.1.6) (García-Vilas & Medina, 2018). HGF/c-Met signaling pathway is one of the essential pathway

playing role in invasion, motility, cell proliferation, angiogenesis and protecting cells from apoptosis (García-Vilas & Medina, 2018). D'Amico et al. demonstrate that inhibition of c-Met on the cancer stem cells in renal tumors inhibited the bone metastasis *in vivo* (Godio et al., 2016).

1.5 Metastatic Models

There are non-animal and animal models to study metastasis. Non-animal models are classified as *in vitro* and *in silico* models, *in vivo* non-animal models.

1.5.1 Non-animal models

1.5.1.1 *In vitro* and *in silico* models

Cell cultures are basic models to investigate the role some proteins in metastasis. The role of chemokine CXCL12 was investigated after performing migration assay of ovarian cancer cells. EMT is indicated by immunofluorescence staining of E-cadherin, vimentin *in vitro*. In addition, co-culture systems are used for finding out the interplay between tumor cells and stromal cells. *In silico* models are also used for analysis of metastasis based on results derived from experiments (van Marion, Domanska, Timmer-Bosscha, & Walenkamp, 2016). For *in vitro* organ specific metastasis models, transwells are used as a cheaper and time-saving method. However, these systems do not completely represent the metastasis because the cells are in a static environment and there is no endothelial barrier (Kong et al., 2016). Cell culture in 2D monolayer is the most common cell culture system. It is less costly when compared to animal models and 3D cell culture systems. However, 3D cell culture mimics *in vivo* biological systems better than 2D cell culture (Li, Tang, & Hou, 2012).

1.5.1.2 *in vivo* Non-animal Models

Beaucher et al. used the *Drosophila melanogaster* to study on the role of MMPs in the initiation of metastasis *in vivo*. Zebrafish is also used for orthotopically xenograft transplantation studies and metastasis of tumor cells is easily imaged due to their transparent embryos (van Marion et al., 2016)

1.5.2 Animal Models

Immunodeficient animal models are necessary for implantation of human derived tumor cells to animals. However, immune cells play role in both elimination of cancer cells in the circulation and progression of tumor such as supporting extravasation of cancer cells (van Marion et al., 2016). Study of metastasis on animal models is performed by injection of cancer cells intravenously, subcutaneously, or orthotopically to immunosuppressive mice (Li et al., 2012).

1.6 Microfluidic Approaches for Mimicking Tumor Microenvironment and Metastasis *in vitro*

Recently microfluidic systems are used for metastasis and drug screening studies. Microfluidic system in other words Lab-on-a-chip (LOC), also called as micro total analysis system (μ TAS), started in the 1990s and provides opportunity to study 3D culture system for many applications such as cell culture, tissue engineering, intracellular signaling, multidrug resistance, drug screening.

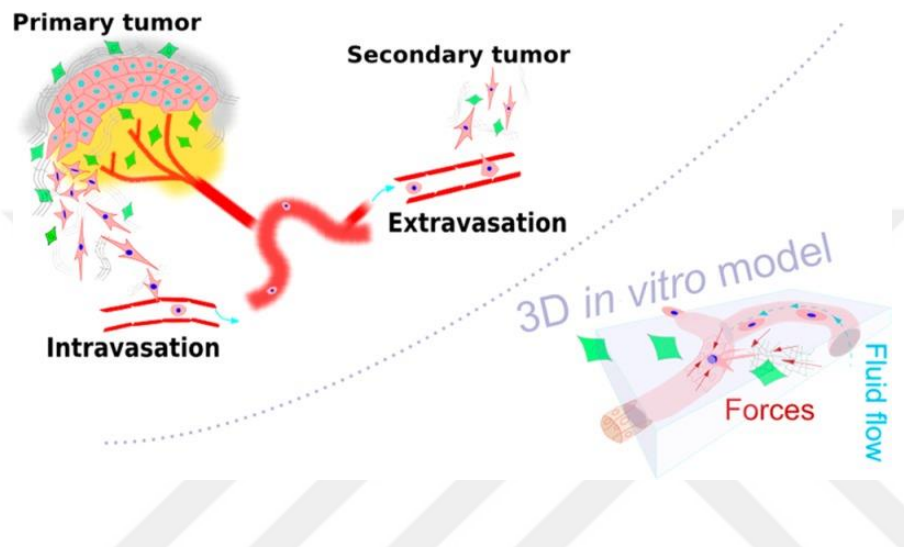


Figure 1.7 Microfluidic Systems. Development in the 3D cell culture system involves mechanical changes in cells for metastatic studies (Malandrino, Kamm, & Moendarbary, 2018).

1.6.1 Lab-on-a-chip (LOC)

Common drug screening models are nonproductive due to incompatible results obtained between (a) 2D cell culture system and *in vivo* and (b) origin difference between animal models and human. Development in the 3D cell culture system *in vitro* models will provide more compatible results and relevance in physiology for drug screening and cancer research (Ahn et al., 2017). Microfluidic system is also used to mimic metastasis of cancer cells to distant organs as liver, lung and bone (Mi et. al, 2016). Microfluidic devices simulate tumor microenvironment better which containing biochemical and mechanical parameters to study extravasation, cell migration and drug screening (Fig.1.7) (Caballero et al.,2017). Microfluidic devices are physiologically relevant to metastasis due to presence of different cell types in 3D cell culture system and they take into account biochemical, mechanical and cellular signals. (Ma, Middleton, You, & Sun, 2018). Tumor microenvironment (TME) is composed of stromal cells like carcinoma-associated fibroblasts (CAFs), endothelial cells and immune cells; growth factors and inflammatory cytokines, and extracellular matrix proteins (Capece et al., 2013). Therefore, mimicking the TME is difficult and current organ-on-a-chip approaches study on

the interplay between tumor and TME. Some of them are listed as tumor-stromal interactions on a chip, tumor-vasculature interactions on a chip, tumor interactions with non-cellular components on a chip (Ahn et al., 2017). Numerous lab-on-a-chip (LOC) devices are designed for studying on each step of metastasis. For instance, Kim et al. demonstrated the migration of MDA-MB-231 cells in the microfluidic 3D system by induction of EGF and SDF-1 α which are secreted stromal cells. Song et al. studied the intravasation of MD-MB-231 cells by means of CXCL12-CXCR4 binding to the endothelial cells on the microfluidic 3D system. Zhang et al. shown that the presence of CXCL12 induces the extravasation of cancer cells over the endothelial barrier as HUVEC on the microfluidic system. Usage of AMD3100 which is inhibitor of CXCR4 blocks the extravasation of cancer cells. Moreover, fluid shear stress can have effect on the invasion of cancer cells. Polocheck et al. applied interstitial flow to the different concentration of cells after seeding of MDA-MB-231 cells on the collagen. They found out that it was based on CCR7 signaling pathway at low concentration of seeding cells (Hsieh-Fu, Alen, Q., & Gang, 2017). Microfluidic system has many advantages that small amount and volume of sample is needed therefore it is cost-effective. Polydimethylsiloxane (PDMS) usually used for LOC systems is pervious to O₂ and CO₂ which is essential for cell growth. PDMS is made of silicone and transparent which enables optical imaging (Sleeboom, Eslami Amirabadi, Nair, Sahlgren, & den Toonder, 2018). Microfluidic system combines cell culture, cell sampling, fluidic control on a single device (Li et al., 2012). Cancer-on-a-chip (CoC) devices are small in size as micrometer to millimeter. Presence of microchannels enables the flow control and control of biochemical, mechanical forces. Moreover, co-culture of different cell types in the same microenvironment provides to simulate human tumor on a single device (Sleeboom et al., 2018). In the context of TUBITAK 1003 project #115E056 Extravasation LOCs were fabricated by Assoc. Prof. Dr. Devrim Pesen Okvur and her group at Izmir Institute of Technology (IZTECH) and the validation of these LOCs for HCC cells were performed by Prof. Dr. Neşe Atabey and her group at Izmir Biomedicine and Genome Center. In this thesis Project, Lab-on-chip device was used to mimic the extravasation of HCC cells as SNU-449 having constitively active c-Met and SNU-398 cells which were absent c-Met in 3D cell culture system to investigate the role of c-Met on the organ specific extravasation. LOC is composed of three channels as medium channel, homing channel and circulation channel. Homing cells were THLE-2 as representing liver epithelial cells, HS-27A as representing bone marrow/stroma cells and BEAS-2B as representing lung epithelial cells. HUVEC cells were used to mimic the endothelial barrier and SNU-449 and SNU-398 cells were used to simulate the circulating tumor cells. All cells had fluorescence proteins and the extravasation was

determined under fluorescence and confocal microscope. As a result of this thesis, it was aimed to determine that the role c-Met on the extravasation and organ specific extravasation in HCC cells via Lab-on-a-chip device.



2. MATERIALS AND METHODS

2.1 Type of Study

It was an experimental study.

2.2 Time and Location of Study

All experiments were performed at Izmir Biomedicine and Genome Center, between 2016 and 2019.

2.3 Population of Study

SNU-449, SNU-398 HCC cell lines, THLE-2, BEAS-2B and HUVEC cell lines were used in this study. After transduction process, generated SNU-398-CMV-GFP and SNU-398-MET as HCC cell lines and THLE-2 mCherry, BEAS-2B mCherry, HS-27A mCherry polyclonal cells were used in this study.

2.4 Cell Culture and Splitting

2.4.1 Culturing HCC Cell Lines

All HCC cell lines were provided by Prof. Dr. Mehmet Öztürk at Izmir Biomedicine and Genome Center. These cells were grown in the presence of complete DMEM or RPMI obtained after adding 10% FBS, 1% Penicilin/Streptomycin, 1% L-Glutamine ve 1% Nonessential amino acids components. The whole process took place under the laminar flow cabinet and the cells were incubated at 37°C, 5% CO₂, 95% humidified incubator. Usually, when the cell confluency was 70%-80%, they were washed with 1x PBS then they were treated with 0,25 % Trypsin/EDTA. The cell culture plate was placed at 37 °C, 5% CO₂, 95% humidified incubator until the cells were detached. The enzyme activity of Trypsin/EDTA was inactivated by adding complete medium which contains FBS in the amount of threefold of Trypsin/EDTA. Depending on the growth rate of cells and cell types, the cells were splitted into cell culture plates or flasks.

2.4.2 Culturing THLE-2 Cell Lines

For this study, BEGM Bronchial Epithelial Bullet kit and BEBM medium (CC-3171+CC-4175), katalog #CC-3170, Lonza) were used for culturing THLE-2 cells. For complete medium preparation, 44.5 ml BEBM, 50 µL Hydrocortisone, 50 µl hEGF, 50 µl Transferin, 50 µl insulin, 50 µl retinoic acid, 50 µl Triiodothyronine, 200 µl Bovine Pituitary Extract, 12.5 µl EGF from 20 µg/ml stock, 3.5 µl phosphoethanolamine, 5 ml FBS were mixed. T-25 cell culture flasks were coated with coating medium which was prepared with 100 µL from 1 mg/ml Fibronectin,

96.8 µl from 3 mg/ml Collogen type, 10 µl from 10 mg/ml BSA and 10 ml BEBM. 400µl coating medium was placed into the T-25 flasks and the flasks were hit by hand so as to cover whole surface of the flask. The flasks were placed at 37 °C, 5% CO₂, 95% humidified incubator overnight. Then the flasks could be stored at 4°C until one month. After the coating medium was aspirated in the flasks, THLE-2 cells were seeded. THLE-2 cells were splitted 1:3 once a week after detaching with 750µl of 0.25% Trypsin-EDTA. Inactivation of Trypsin-EDTA was done by adding complete THLE-2 medium and the cells were centrifuged at 200xg for 5 minutes and the pellet was dissolved and splitted into the coated T-25 flasks at 1:3 ratio. Freezing medium of THLE-2 cells contained 30% FBS, 10% DMSO and 60% complete medium.

2.4.3 Culturing BEAS-2B Cell Lines

For this study, BEGM Bronchial Epithelial Bullet kit and BEBM medium (CC-3171+CC-4175), katalog #CC-3170, Lonza) were used for culturing BEAS-2B cells. For complete medium preparation, 49.4 ml BEBM, 50 µL Hydrocortisone, 50 µl hEGF, 50 µl Transferin, 50 µl insulin, 50 µl retinoic acid, 50 µl Triiodothyronine, 200 µl Bovine Pituitary Extract, 50 µl Epinephrine. T-25 or T-75 cell culture flasks were coated with coating medium which was prepared with 100 µL from 1 mg/ml Fibronectin, 96.8 µl from 3 mg/ml Collogen type, 10 µl from 10 mg/ml BSA and 10 ml BEBM. 400µl coating medium was placed into the T-25 and 750µl for T-75 flasks and the flasks were hit by hand so as to cover whole surface of the flask. The flasks were placed at 37 °C, 5% CO₂, 95% humidified incubator overnight. Then the flasks could be stored at 4°C until one month. After the coating medium was aspirated in the flasks, BEAS-2B cells were seeded. BEAS-2B cells were splitted when their confluency was 70% because they would differentiated unless they were not subcultured. Cells were detached with 0.25% Trypsin-EDTA containing 0.5% Poly(vinylpyrrolidinone) (PVP) which was prepared with 10 ml of %0.25 Tripsin-EDTA and 0.05 gram PVP. After vortexing very well, the solution was filtered with 0.2 micron filter. Inactivation of Trypsin-EDTA was done by adding complete BEAS-2B medium and the cells were centrifuged at 200xg for 5 minutes and the pellet was dissolved and splitted into the coated flasks. Freezing medium of BEAS-2B cells contained 1% PVP in the complete medium and 7.5% DMSO.

2.4.4 Culturing HS-27A Cell Lines

Gibco RPMI Medium 1640 (1x), Ref no: A10491-01, Lot: 1854880 was used to culture HS-27A cells. Complete medium contained 10% FBS, 1% L-Glutamine, 1% Non-essential amino acids. Due to absence of Pen-Streps, laminar flow cabinet was sterilized through 1 hour by UV.

After detaching with 0.25% Trypsin-EDTA, inactivation of Trypsin-EDTA was done by adding complete HS-27A medium. The cells were splitted into the flasks at 1:4 ratio once a week. Freezing medium of HS-27A cells contained 30% FBS, 10% DMSO and 60% complete medium.

2.4.5 Culturing Human umbilical vein endothelial cell (HUVEC) Cell Lines

Lonza EBM-2 medium with catalog number CC31-56 and Lonza EGM-2 SingleQuots bullet kit with catalog number CC-4176 were mixed according to the manufacturer's' instructions and the complete medium contained 20% FBS. T-25 cell culture flasks were coated with coating medium which was prepared with 10 μ L from 1 mg/ml Fibronectin and 1 ml BEBM. 400 μ l coating medium was placed into the T-25 which were hit by hand so as to cover whole surface of the flask. The flasks were placed at 37 °C, 5% CO₂, 95% humidified incubator overnight. Then the flasks could be stored at 4 °C until one month. After the coating medium was aspirated, HUVEC cells were seeded on the flasks. HUVEC cells were washed with %0.25 Tripsin-EDTA once and then they were treated with 0,25 % Trypsin/EDTA. Inactivation of Trypsin-EDTA was done by adding complete HUVEC medium and the cells were centrifuged at 200xg for 5 minutes and the pellet was dissolved and splitted into the coated flasks. Freezing medium of HUVEC cells included 80% complete EGM-2 medium, 10% FBS and 10% DMSO.

2.4.6 Cell Counting

After the cells were detached via 0,25 % Trypsin/EDTA and inactivation of trypsin, cell suspension was obtained. 100 μ l of Trypan blue solution (0.5 %, *Biological Industries*), 300 μ l of 1x PBS and 100 μ l cell suspension is mixed. 10 μ l of the mix was loaded on Neubauer hemocytometer and the cells on the five squares/areas shown on the **Figure 2.1.** were counted twice and calculation was shown below in detail and the cell number per 1 ml was determined.

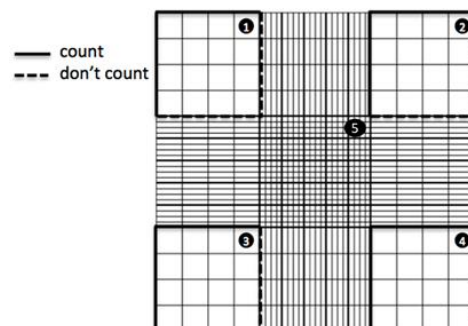


Figure 2.1 Cell counting. The cells on the five squares/areas on Neubauer hemocytometer were counted twice.

1 ml of cells = (total cell number/10 areas)*dilution factor*10⁴

2.4.7 Thawing cells and Freezing the cells

The cells stored at liquid nitrogen in the cryovials were thawed at water bath setting to 37°C. In the laminar flow cabinet, 4 ml of complete RPMI/DMEM and 1 ml of thawing cell suspension was mixed by pipeting in a 15 ml of sterile falcon. The cells were centrifuged at 1500xrpm for 5 minutes. The supernatant was aspirated and the pellet was dissolved in the complete RPMI/DMEM and seeded into the appropriate flask or cell culture plate. The cell culture plate was placed at 37 °C, 5% CO₂, 95% humidified incubator overnight and the cells were splitted until their confluency was reached to 70%-80%.

2.4.8 Freezing Cells

Medium on the cells were aspirated and they are washed with 1x PBS. After the cells were detached via 0,25 % Trypsin/EDTA and inactivation of trypsin was performed then cell suspension was obtained. The cells were centrifuged at 1500xrpm for 5 minutes. The supernatant was aspirated and the pellet was dissolved in the freezing medium containing 30% FBS, 10% DMSO and 60% complete medium and 1 million of cells/cryovial in 1 ml of freezing medium was added to cryovials. Cryovials were placed into the Mr. Frosty including 100% isopropanol which decreased temperature 1°C/minute at -80°C overnight. Then the cells were stored at liquid nitrogen tank.

2.5 Fluidic Shear Stress Treatment

To apply fluidic shear stress on HCC cell lines Watson Marlow 205U peristaltic pump, Marprene Tube Elements for 2.79 bore Watson Marlow tubing and bubble traps were used (Fig.2.2). After cells were grown on 70% confluency they were washed with 1x PBS then they were treated with 0.25 % Trypsin /EDTA. The cell culture plate were placed at 37 °C, incubator until the cells were detached. The enzyme activity of Trypsin/EDTA were inactivated by adding complete medium which contains FBS in the amount of threefold of Trypsin/EDTA. Cells were counted with hemocytometer and three million cells were loaded in bubble traps in 8ml medium. Peristaltic pump system turned on and placed in the 37 °C, incubator and cells were sheared under 0.5 dyn/cm² FSS as refered to 3.4 rpm, toward counterclockwise. After treatment of FSS for 4 hours the cells were collected from bubble traps and they were counted via trypan blue on hemocytometer threetimes and viability of the sheared cells were detected. After shear stress treatment cells were loaded into Lab-on-a-chip.



Figure 2.2 Fluidic Shear Stress Treatment. Watson Marlow 205U peristaltic pump, Marprene Tube Elements for 2.79 bore Watson Marlow tubing and bubble traps were used.

2.6 Lab-on-a-chip (LOC)

In this thesis Project extravasation LOCs were used. In the context of TUBITAK 1003 project #115E056 Extravasation LOCs were fabricated by Assoc. Prof. Dr. Devrim Pesen Okvur and her group at Izmir Institute of Technology (IZTECH) and the validation of these LOCs for HCC cells were performed by Prof. Dr. Neşe Atabey and her group at Izmir Biomedicine and Genome Center. Extravasation LOCs were placed in the tissue culture dish and they were exposed to UV for sterilization in the laminar flow cabinet through 1 hour. Extravasation LOC was composed of 3 channels as medium channel, homing channel and circulation channel.

2.6.1 Coating of LOCs

Then pure Aceton-2% APTES solution was prepared freshly and the solution was loaded from the circulation channel and it should have coat all the channels. The LOCs were held for 15 minutes in the laminar flow cabinet until all liquid evaporated. The LOCs were washed with 1x PBS three times and once with ultra pure dH₂O. 0.0125 mg/ml laminin in 1x universal buffer was prepared and it was loaded to LOCs from circulation channel. The LOCs were placed into Schifferdecker staining jar (catalog number 073.03.001) as the circulation channel down in position at 37 °C, 5% CO₂, 95% humidified incubator for 1h. After that the channels were washed with 1x universal buffer and ultra pure water three times respectively. The LOCs were placed in the glass petri dishes and incubated at the vacuum

desiccator which was used to completely remove water traces and dried the LOCs in a week (Fig.2.3).



Figure 2.3 Vacuum Desiccator

2.6.2 Loading of Homing Cells and HUVEC Cells

Matrigel was held on the ice at +4 °C overnight so as to quite slowly thaw the matrigel the day before. Pipette tips were holded at -20°C the day before. Homing cells as HS-27A mCherry polyclonal, THLE-2 mCherry polyclonal and BEAS-2B mCherry polyclonal cells were detached via trypsin and counted hemocytometrically by Neubauer hemocytometer. These cells were mixed with matrigel (8 mg/ml) at 1:1 ratio as 300,000 cells/100µl HS-27A and BEAS-2B; 600,000 cells/100µl THLE-2. These cell numbers were optimized in the context of the TUBITAK Project. The LOCs were placed into Schifferdecker staining jar as homing channel position in down. They were incubated at 37 °C, 5% CO₂, 95% humidified incubator for 30 minutes results in matrigel polymerization. Human umbilical vein endothelial cells (HUVECs) were endothelial cells that were used to simulate the endothelial barrier during extravasation. They were stained with 5µM Green Cell Tracker (*CellTracker™ Green CMFDA Dye, catalog number C2925, Thermo Fisher Scientific*) in serum-free medium in the 6 cm tissue culture dish for 45 minutes at 37°C, 5% CO₂, 95% humidified incubator. Then the dye was inactivated by adding complete RPMI which contained FBS. Cells were centrifuged at 200xg for 5 minutes. Supernatant was aspirated and cells were dissolved in the 8% Dextran in EGM medium as 3.8 million cells/ml. Dextran was used to increase viscosity of liquid HUVEC cells were loaded into circulation channel and LOCs were placed into Schifferdecker staining jar as medium channel down in position. Therefore, only the posts extravasation taken place were coated. LOCs were incubated at 37 °C, 5% CO₂, 95% humidified incubator overnight. LOCs were imaged under the confocal microscope whether the HUVEC cells coated the post surface or

not. The image was taken as Z-stack so as to verify HUVEC cells completely coating the depth derived from matrigel.

2.6.3 Loading of SNU-449 Azurite Monoclonal Cells

In this study, we used HCC lines SNU-449, SNU-398 in terms of c-Met expression and activation level. Fig.2.4 shows that SNU-449 cells had high c-Met activation and expression. SNU-398 cells had no c-Met activation and low/no c-Met expression by western blot (Unpublished data, Atabey, N.). SNU-449 Azurite monoclonal cells were grown in the complete RPMI containing 10% FBS until passage number of three. SNU-449 Azurite cells were cultured 5% FBS containing RPMI and DMSO to mimic control group and 2.500 nM SU11274 to inhibit c-Met receptor was added the day before. The dose of SU11274 was optimized by Atabey Laboratory via western blot and this dose did not kill the cells which was the lowest dose inhibiting the activation of c-Met. Next day, SNU-449 Azurite cells were detached and cell suspension was prepared. 100.000 cells/ml SNU-449 Azurite cell suspension was prepared. Prepared cell suspension was loaded into circulation channel and 1st day image was taken via confocal and fluorescence microscope as tile scan and 2D images. LOCs were incubated for 7 days as medium channel down Schifferdecker staining jar and the images were taken at day0, day2, day5 and day7 so as to view extravasation of SNU-449 Azurite cells to homing cells in the form of tile scan and 2D images. The extravasated posts were determined at the end of 7th day and extravasation and organ specific extravasation of SNU-449 Azurite cells was analyzed via Microsoft Excel and Graphpad Prism. Follow up paper which was attached to appendix was used for determination of extravasation+/- posts for each LOC. Experimental design for loading of SNU-449 Azurite cells to Lab-on-a-chip was described (Fig.2.5). After seven day incubation, LOCs were fixed with 4% PFA at 4°C overnight. Then the LOCs were washed with 1x PBS twice and they were stored at 4°C.

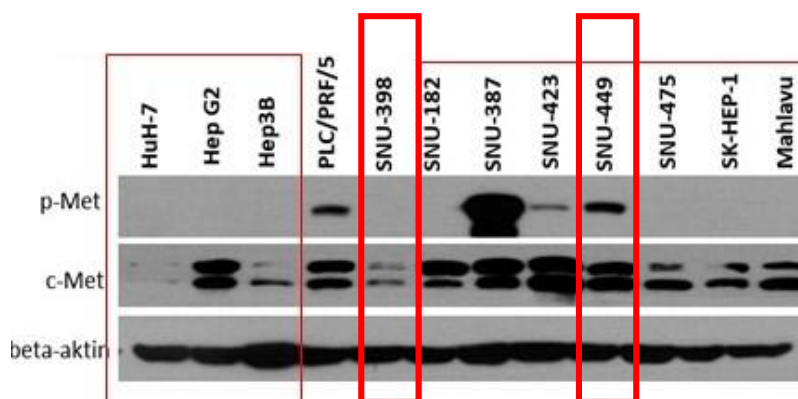


Figure 2.4 Western blot result of c-Met expression and activation of SNU-449 and SNU-398 cells (Unpublished data, Atabey N.).

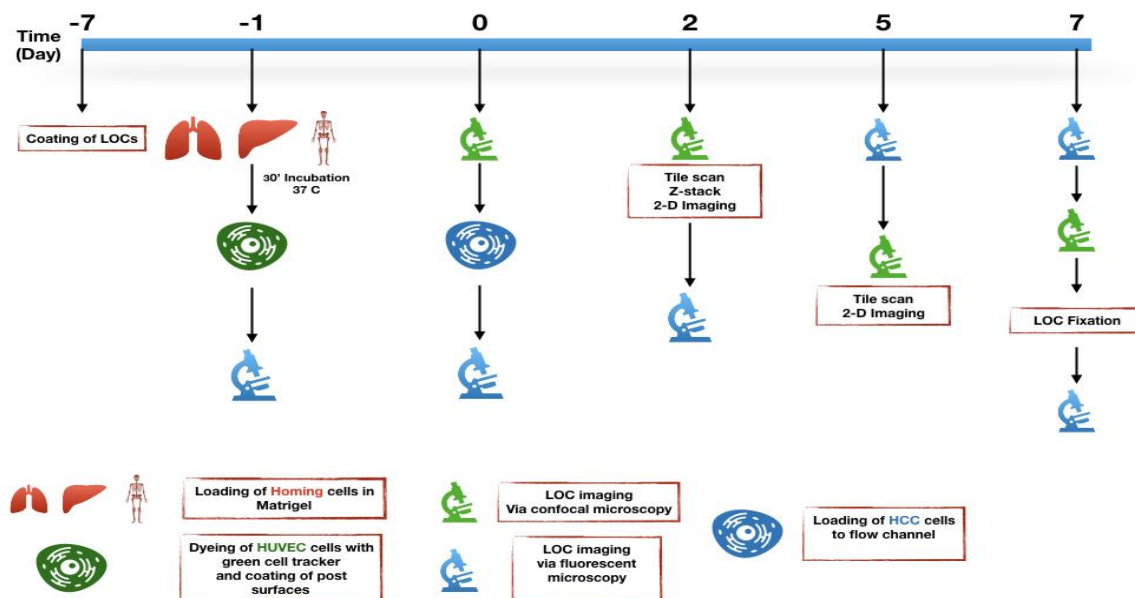


Figure 2.5 Experimental Design for loading of SNU-449 Azurite cells to Lab-on-a-chip

2.6.4 Loading of SNU-398 CMV GFP (MOCK) and SNU-398 MET GFP Overexpressed Cells

The protocol for loading of SNU-398 cells was a little different from loading of SNU-449 Azurite cells. SNU-398 CMV GFP (Mock) and SNU-398 MET GFP Overexpressed cells had green color. Therefore, HUVEC cells were loaded into circulation channel without any staining. SNU-398 CMV GFP (Mock) and SNU-398 MET GFP Overexpressed Cells' color was not so intense therefore they were stained with 5 μ M Green Cell Tracker (*CellTracker™ Green CMFDA Dye, catalog number C2925, Thermo Fisher Scientific*) in serum-free medium in the 6 cm tissue culture dish for 45 minutes at 37°C, 5% CO₂, 95% humidified incubator. Then the dye was inactivated by adding complete RPMI. Cells were centrifuged at 1500rpm for 5 minutes. Supernatant was aspirated and 100,000 cells/ml SNU-398 CMV GFP (Mock) and SNU-398 MET GFP Overexpressed cells were prepared. Prepared cells suspension was loaded into circulation channel and 1st day image was taken via confocal and fluorescence microscope as tile scan and 2D images. LOCs were incubated for 7 days as medium channel down Schifferdecker staining jar and the images were taken at day0, day2, day5 and day7 so as to view extravasation of SNU-449 Azurite cells to homing cells in the form of tile scan and 2D images. The extravasated posts were determined at the end of 7th day and extravasation and organ specific extravasation of SNU-398 CMV GFP (Mock) and SNU-398 MET GFP Overexpressed cells was analyzed via Microsoft Excel and Graphpad Prism. Follow up paper which was attached to appendix was used for determination of extravasation+/- posts for each

LOC. After seven day incubation, LOCs were fixed with 4% PFA at 4°C overnight. Then the LOCs were washed with 1x PBS twice and they were stored at 4° C.

2.7 Protein Isolation

When the confluency of cells reached %70, medium on the cells was aspirated and they were washed with cold 1x PBS containing 0.1 mM Na₃VO₄, 0.1mM NaF twice on the ice. After adding 1 ml of the PBS on the cells, the cells were scraped with a sterile scraper. Cells were collected into a sterile eppendorf and they were centrifuged at 2500 rpm at 4 °C for 5 minutes. The supernatant was aspirated and the pellet was stored at -80 °C until proteins were isolated. Depending on the pellet, the appropriate amount of RIPA buffer (Radioimmunoprecipitation), usually threefold of pellet, which contains 150mM NaCl, 1% NP-40, 50mM Tris-Cl pH 7.4, EDTA pH 8.0, 1X protease inhibitor cocktail (Roche), 1mM Na₃VO₄, 1mM NaF was added on the pellet. The pellet was vortexed every 10 minutes through 30 minutes on ice. After that, in order to increase the lysis of the cells, 10 seconds sonication was performed three times. Subsequently, the eppendorfs were centrifuged at 15,000xg at +4°C for 30 minutes. The supernatant included proteins were transferred into a new eppendorf. The concentration of proteins were determined via BCA protein assay kit.

2.7.1 BCA (Bicinchoninic Acid) Protein Assay

The principle of BCA assay was based on reduction of Cu²⁺ to Cu¹⁺ in the presence of cysteine or cystine, tyrosine, and tryptophan aminoacids in the alkaline solution resulted in purple color. Different concentration of BSA (Bovine Serum Albumin) were used so as to create standard graphs. Mix of BCA reagent A and B (50:1) was added on the protein lysate. The reaction took place at 55°C for 15 minutes or at 37°C for 30 minutes in the dark. The more amount of protein was, the more purple color was. The photometric measurement was performed by Varioscan machine at 562 nm. The concentration of proteins was determined based on equation derived from the standard graph. Depending on the calculation obtaining from the standard graph, the eppendorfs containing proteins (50 µg-70 µg), 20% beta-mercaptoethanole, 4x Laemmli buffer as loading dye were boiled at 95°C for 10 minutes so as to denature the proteins.

2.7.2 SDS-PAGE (Polyacrylamide gel electrophoresis)

Polyacrylamide gel composed of 10% resolving gel and 5% stacking gel was prepared. Based on the molecular weight of desired protein the concentration of resolving gel was alterable. Therefore, for proteins having small molecular weight 8%-12% or 8%-15% resolving gel was prepared. 7 ml of resolving gel was poured into the system setting before including glasses. Adding 80% isopropanol on the gel so as to provide oxygen-free environment for

polymerization. After polymerization of resolving gel and removing isopropanol, 3 ml of stacking gel was poured in the resolving gel and subsequently 10 cm, 10-well comb was placed into the gel. After polymerization of the gel, the gel could be stored in the running buffer at +4°C in a week. Electrophoresis tank was filled with 1x running buffer. After removing the comb, the gel was placed into the tank then 3 µl of pre-stain protein marker and denatured protein samples were loaded into the well one by one. The proteins were exposed to 70 volt firstly, the volt was set to 110 volt after loading dye passing the stacking gel. After the electrophoresis run was completed, the gel was removed from the glass and holding in the 1x transfer buffer. PVDF membrane (millipore) and whatman paper was cut as 8cmx6cm and 9cmx7cm in size respectively. PVDF membrane was incubated in the %100 methanole for 1 minute in order to open the pores. The membrane and wattman paper was hold in the transfer buffer. For wet transfer process, black side of tray is placed down then respectively whatmann paper, gel, membrane, whatmann paper, sponge was placed to form a sandwich in the transfer buffer (Fig. 2.6) . The bubbles which prevents transfer of proteins were removed by a roller. Then, the tray was closed and placed into the tank filled with 1X transfer buffer. Transfer took 3 hours at 400 milliAmper (mA) at RT on magnetic stirrer. In order to prevent excessive warm due to high current, an icepack was placed into the tank and magnetic stirring bar was also placed in the tank so that current could be equally distributed through the system. After transfer was completed, the membrane was incubated in the %100 methanole for 1 minute, in the ultrapure water for 1 minute and in the 1x TBS for 2 minutes. Membrane was rotated in the falcon tube for 1 hour at RT in the blocking solution %5 BSA in 1X TBS. Blocking was done so as to prevent the binding of antibody to non-specific region. After blocking, the membrane was incubated by rotating in the primary antibody solution (%3 BSA in the %0,2 TBS-T, %0,1 primary antibody) at +4°C overnight in the falcon tube. The membrane was washed with %0,1 TBS-T solution threefold for 5 minutes by rotating on the following day. Based on the primary antibody is used, the proper infrared secondary antibody was prepared. The membrane was incubated in the secondary antibody in the ambertube (SPL) having dark color to prevent light transmittance for 2 hours at RT by rotating on the Roto-shake genie (*Scientific Industries*). The membrane was washed with %0,1 TBS-T solution four times for 5 minutes, once with 1x TBS solution so as to remove the detergent on the membrane before imaging. Membrane was imaged via LI-COR Odyssey Clx infrared fluorescence imaging system containing two different fluorescent channels as 700 nm and 800 nm wavelength. Finally, densitometric analysis of proteins band was performed by ImageJ programme.

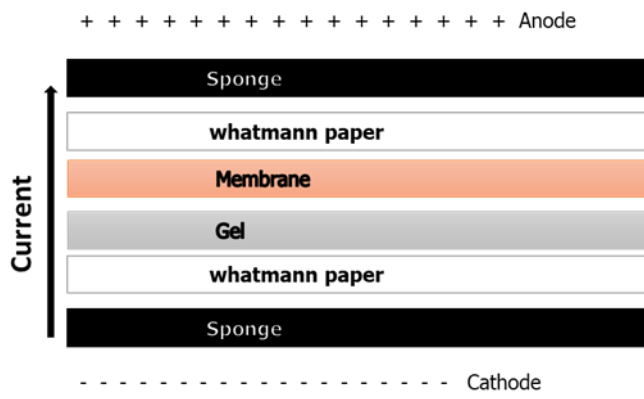


Figure 2.6 Organization of sandwich system for transfer of proteins from gel to PVDF membrane.



2.8 MATERIALS

2.8.1 Preparation of Solution

2.8.1.1 Solution for Western Blot

1.5 M Tris pH 8,8 (100 ml); 18,165 gram Tris was dissolved in the 60 ml ddH₂O then pH was set to 8,8 by adding HCl and volume was completed to 100 ml by adding ddH₂O.

1 M Tris pH 6,8 (100 ml); 12,11 gram Tris was dissolved in the 60 ml ddH₂O then pH was set to 6,8 by adding HCl and volume was completed to 100 ml by adding ddH₂O.

30% Acrylamid-Bisacrylamid Solution: 29 gram of acrylamid and 1 gram of bisacrylamid was dissolved in 60 ml ddH₂O very well then the volume was set to 100 ml by adding ddH₂O. Homogeneous mix was filtered via 0,2 µM filter and stored at +4°C in the dark.

1X TBS: 4 gram NaCl, 0.1 gram KCl, 1.5 gram Tris was dissolved in the 400 ml ddH₂O water and pH was set to 7.4 then the volume was completed to 500 ml by adding ddH₂O.

1X TBS-T : 500 ml TBS and 500 µl Tween-20 was mixed to generate %0.1 TBS-T.

Running Buffer : 14.4 gram Glisin, 3.075 gram Tris and 10 ml 10% SDS was mixed. The volume was set to 1 liter via ddH₂O. The buffer was stored at +4°C.

Transfer Buffer: 14.4 gram Glisin, 3.075 gram Tris and 2 ml 10% SDS was mixed. 800 ml of ddH₂O was added and mixed very well. The volume was set to 1 liter via adding methanol before use. The buffer was stored at +4°C.

10% APS (Ammonium Persulfate): 0.1 gram APS was mixed with 1 ml of ddH₂O.

10% NaN₃ (Sodium Azide): 1 gram NaN₃ was mixed with 10 ml of ddH₂O.

Coomassie Blue Staining Solution: 100 ml methanol, 80 ml ddH₂O, 20 ml acetic acid and 0.1 gram Coomassie R250 Blue was mixed very well and stored at RT in the light-tight bottle.

Resolving Gel (10%): 4 ml dH₂O, 3.3 ml 30% Acylamid-Bisacrylamid solution, 100µl 10% SDS, 2.5 ml 1.5 M Tris(pH 8,8) were mixed very well. Then 100 µl 10% APS and 4µl TEMED was added.

Stacking Gel(5%): 2.1 ml dH₂O, 0.5 ml 30% Acylamid-Bisacrylamid solution, 30µl 10% SDS, 380µl 1M Tris(pH 6,8) were mixed very well. Then 30µl 10% APS and 3µl TEMED was added. The mix was poured on the resolving gel.

RIPA Lysis Buffer : 50 mM Tris (pH 7.4), 150 mM NaCl, 1mM EDTA (PH 8) and 1% NP40 solutions were mixed and the volume is completed to 100 ml by adding dH₂O. Before use, 1 mM Na₃VO₄, 1 mM NaF and 1 tablet protease inhibitor cocktail (*Complete ULTRA Tablets Mini, EASYpack, Protease Inhibitor Cocktail Tablets, Roche*) was added to 10 ml Lysis buffer.

Primary Antibody Preparation: 3% BSA, 0.02% Tween-20 and 1:1000 primary antibody was mixed in 1X TBS.

Secondary Antibody Preparation; 3% BSA, 0.02% Tween-20, 0.01% SDS(10%), 1:20000 Secondary antibody in 1X TBS. Moreover, 0.02% NaN₃ (10%) was added to secondary antibody.

Table 2.1 Lists of Equipment used

Equipment	Brand	Catalog Number
CO2 Incubator	Memmert	Inco 153
PH Metre	HI 221	Hanna
Vortex	Thermo Scientific	88880018
Peristaltic Pump	Watson Marlow	205U
Water bath	Nüve	NB 9
Odyssey CLx Infrared Imaging System	LI-COR	
Western Blotting Transfer System	Bio-Rad	1658029
Sonicator Bioruptor Pico	Diagenode	B01060001
Desiccator	Isolab	I.039.12.200
Neubauer Hemocytometer	Marienfield Superior	0630010
Inverted Microscope for Advanced Routine	Carl Zeiss	Axio Vert.A1
mySPIN™ 6 Mini Centrifuge	Thermo Scientific	75004061
Sartorius™ Entris™ Toploading Balances	Sartorius	8221S
SimpliAmp Thermal Cycler	Thermo Scientific	A24811
Safe 2020 Class II Biological Safety Cabinets	Thermo Scientific	51026638
Roto-Shake Genie	Scientific Industries	SI-1100
Centrifuge 5810 R	Eppendorf	5810 R

Magnetic Stirrer C-MAG MS 10	IKA	0003582600
MicroCL 17R Microcentrifuge	Thermo Scientific	75002450
Gel Doc™ XR+ Gel Documentation System	BIO-RAD	1708195
Motorized Upright Fluorescence Microscope	Olympus	BX61-32FA1-S08



3. RESULTS

3.1 Homing Cells were transduced with plasmids containing mCherry tagged fluorescent protein with lentivirus

THLE-2 as representing liver epithelial cells, HS-27A as representing bone marrow/stroma cells and BEAS-2B as representing lung epithelial cells were used as homing/target tissue for predicting extravasation of SNU-449 and SNU-398 HCC cell lines. Therefore, THLE-2, BEAS-2B and HS-27A cells were transduced with plasmid containing mCherry tagged fluorescent protein with lentivirus and they were permanently expressed mCherry fluorescent proteins so as to easily be visualized under the microscopy (Fig. 3.1). Figure 3.1 shows their fluorescent and DIC images under the 10X objectives.

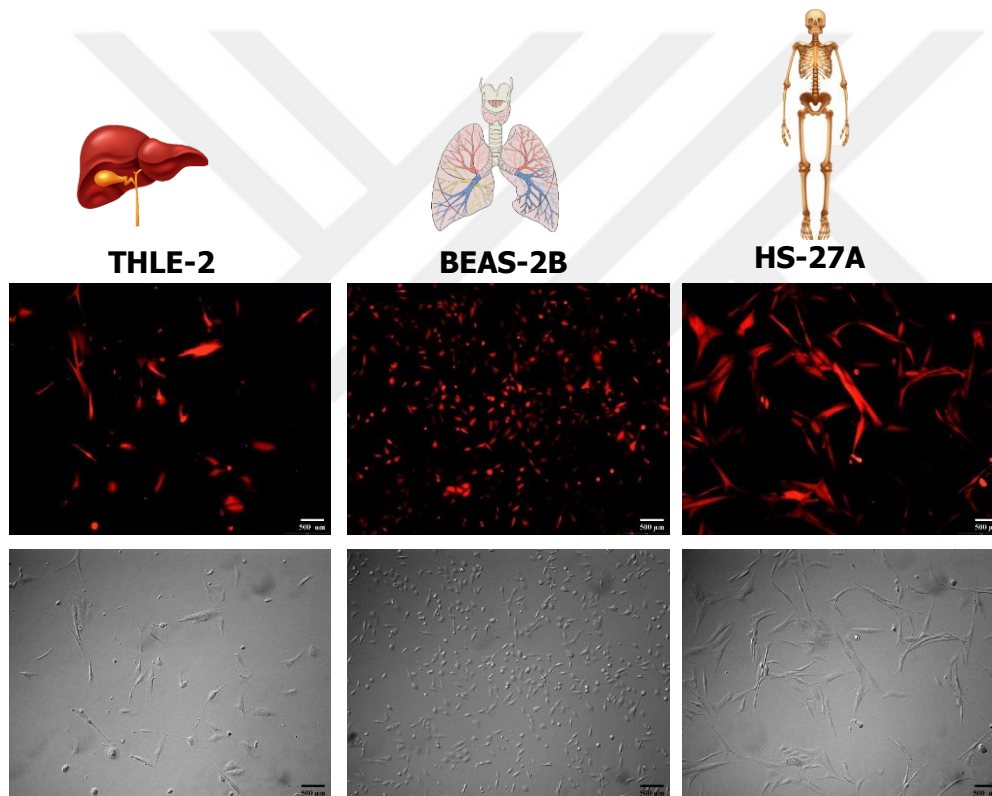


Figure 3.1 The top images were fluorescent images of THLE-2 mCherry polyclonal cells as representing liver epithelial cells, BEAS-2B mCherry polyclonal cells as representing lung epithelial cells HS-27A mCherry polyclonal cells as representing bone marrow/stroma cells respectively and the bottom images were DIC images of them respectively by using Olympus IX71 Fluorescence microscope under 10X objective via red filter and DIC.

3.2 HUVEC (Human Umbilical Vein Endothelial Cells) cells as representing endothelial barrier stained with CellTracker™ Green CMFDA Dye

HUVEC cells were used for representing endothelial barrier during extravasation of cancer cells *in vitro*. HUVEC cells were stained with 5 μM of CellTracker™ Green CMFDA Dye and the green color was not faded during one week incubation (Fig.3.2). Transduction of HUVEC cells were difficult. Therefore, they were stained with 5 μM of CellTracker™ Green CMFDA Dye which was stable and non-toxic to living cells. The dye had ability to pass cell membrane easily and glutathione S-transferase converted chloromethyl/bromomethyl group on the dye and thiol groups into nonpermeable yield. After the conversion of nonpermeable yield, the color was transferred to generations to generations longer than 72 hours.

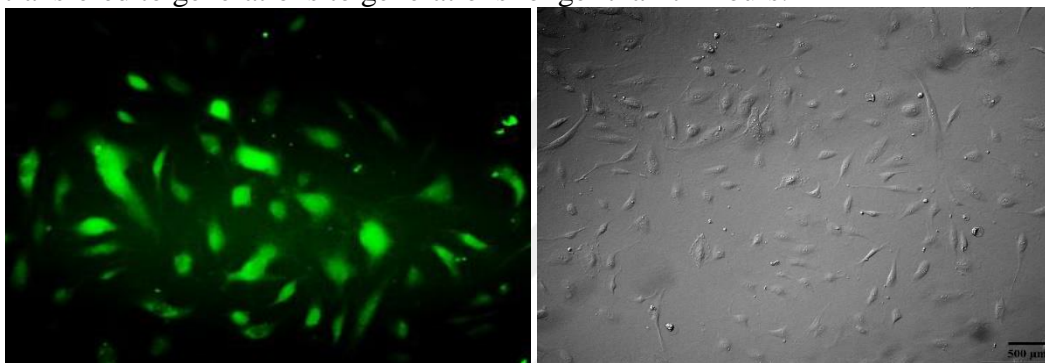


Figure 3.2 HUVEC cells were stained with 5 μM Green Cell Tracker respectively and the bottom images were DIC images of them respectively by using Olympus IX71 Fluorescence microscope under 10X objective via green filter and DIC.

3.3 SNU-449 cells were transduced with plasmid containing Azurite tagged fluorescent protein with lentivirus

SNU-449 had constitively active c-Met and they were used for to investigate the role of c-Met on the organ specific extravasation. Here, they simulated the circulating tumor cells which had constitively active c-Met in the circulation. SNU-449 cells were transduced with plasmid containing Azurite tagged fluorescent protein with lentivirus and they were permanently expressed Azurite fluorescence proteins (Fig.3.3)

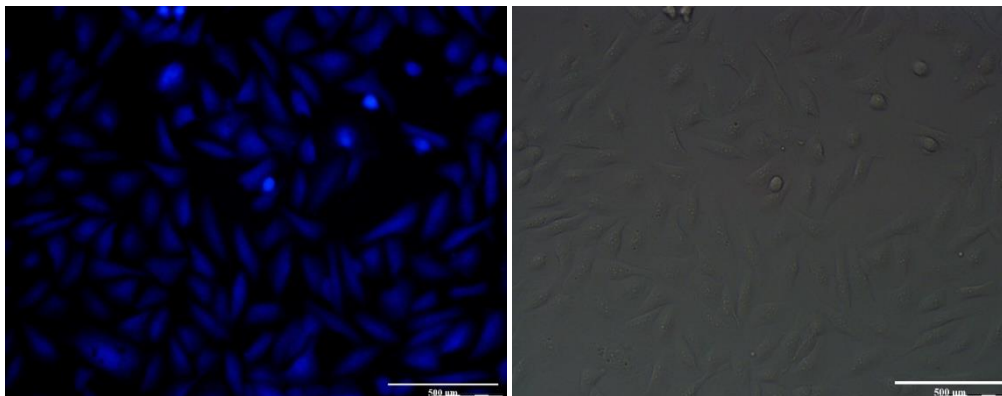


Figure 3.3 Fluorescent and DIC images of SNU-449 Azurite monoclonal cells respectively by using Olympus IX71 Fluorescence microscope under 20X objective via blue filter and DIC.

3.4 Loading of Homing cells to homing channel, HUVEC cells and SNU-449 Azurite monoclonal cells to flow channels on the Extravasation Lab-on-a-chip

In the context of TUBITAK 1003 project #115E056 the protocol of extravasation LOCs were optimized. The coating of the LOCs were performed in accordance with this protocol which were described at material-methods section. After the dehumidification of the coated LOCs were ensured, homing cells were loaded into homing channel of the LOC. THLE-2 mCherry polyclonal cells as liver epithelial cells, BEAS-2B mCherry polyclone cells as lung epithelial cells were loaded on the homing channel of extravasation LOC by mixing with matrigel. The concentration of homing cells were optimized in the context of the Tübitak Project which were described in the material-methods section. Fig.3.4 shows the tile scan images of polymerized matrigel mixed with THLE-2, BEAS-2B and HS-27A cells respectively after incubated at 37 °C %5 CO₂ 95% humidified incubator for 24h. The homing cells were distributed properly and they were completely coated the homing channel to for 3D culture system. They were not overflowed to flow channels and they were intact.

Homing Cells

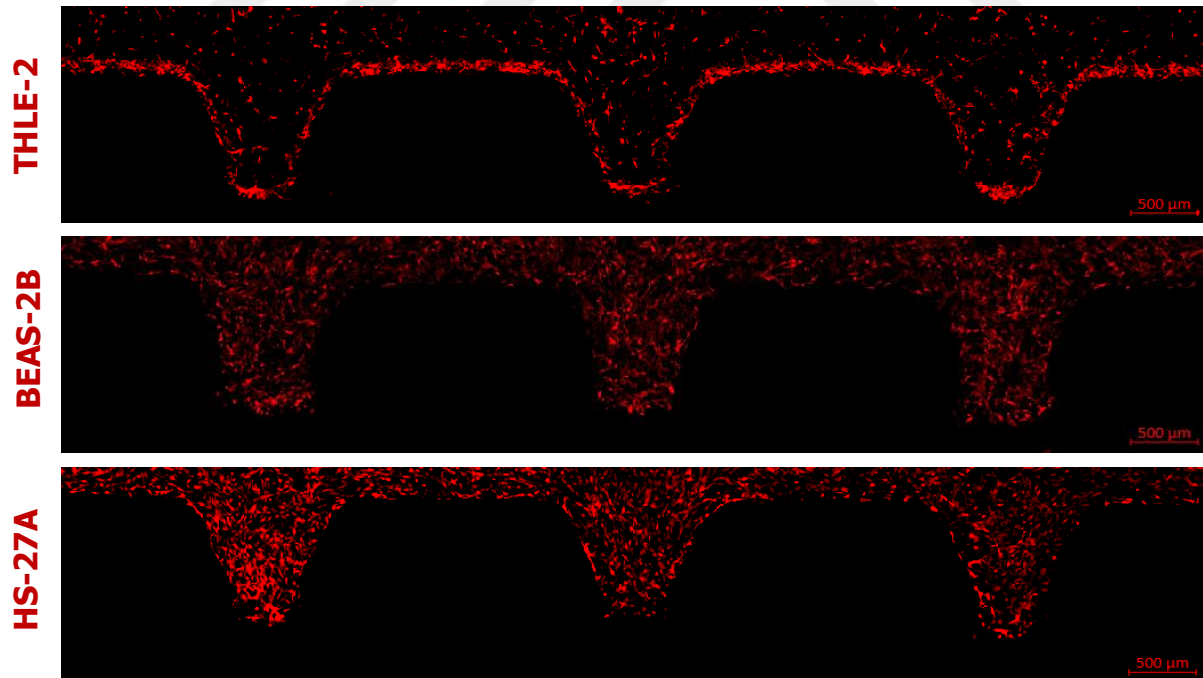
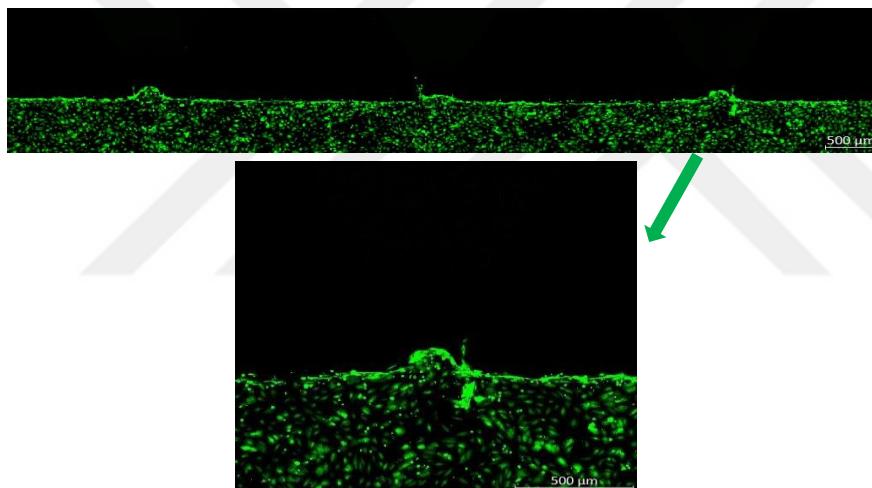


Figure 3.4 Tile scale image of homing channel of extravasation LOC with of THLE-2 (600.000 cells/100µl) , BEAS-2B (600.000 cells/100µl) and HS-27A (300.000 cells/100µl) mCherry polyclone homing cells in matrigel respectively. (The tile scan image was taken under Zeiss LSM 880, Axio Observer microscope at Izmir Biomedicine and Genome Center by using 594 nm laser and 594 nm filter under 5X objective. The image was analysed via ZEN Blue programme).

After polymerization of matrigel which was mixed with homing cells, 3.8 million cells/ml HUVEC cells, the cell number was optimized in the context of the Tübitak Project, was loaded into circulation channel after dissolved in 8% Dextran which was used for increasing viscosity of liquid so as to provide equally distribution of HUVEC cells through circulation channel. Only extravasation post surface was coated with HUVEC. After incubation of the LOCs for 24h, the coating of HUVEC cells through circulation channel was controlled by confocal microscopy via *z-stack*. Only, the LOCs which were completely coated posts that extravasation taken place and completely formed endothelial barrier were used for further steps. The incubation time for extravasation follow-up was seven days and integrity of coated posts that extravasation taken place was maintained though 7 days. Fig.3.5 indicates the integrity of endothelial barrier was maintained for 7 days by confocal microscopy and these images were taken from different LOCs only contained matrigel in the homing channel.

a)



b)

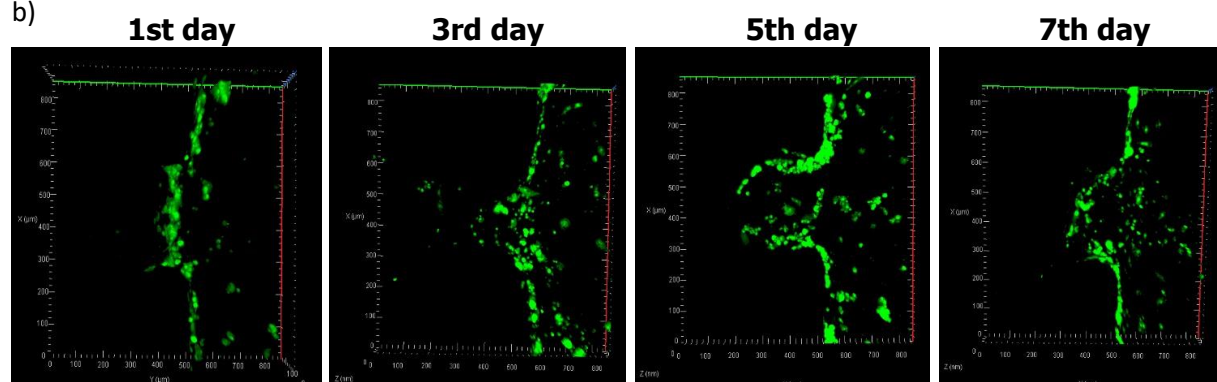


Figure 3.5 a) The first day the tile scan image and post image of HUVEC cells b) The *z-stack* images HUVEC cells stained with Green Celltracker in the circulation channel of extravasation LOC was coated the endothelial barrier through 7 days and the images of 1st, 3rd, 5th and 7th day of HUVEC coating. The *z-stack* image was taken

under Zeiss LSM 880, Axio Observer microscope at Izmir Biomedicine and Genome Center by using 488 nm laser and 488 nm filter under 10X objective. The image was analysed via ZEN Blue programme.

After the formation of endothelial barrier, SNU-449 Azurite monoclonal cells were loaded into circulation channel. In the context of Tübitak Project the loading cell number of SNU-449 was optimized as 50.000 cells-100.000 cells/ml. Figure 3.6 shows that the tile scan image of SNU-449 Azurite monoclonal cells in the circulation channel. The cells were distributed equally through the channel and they were not passed through homing channel, stayed in circulation channel.

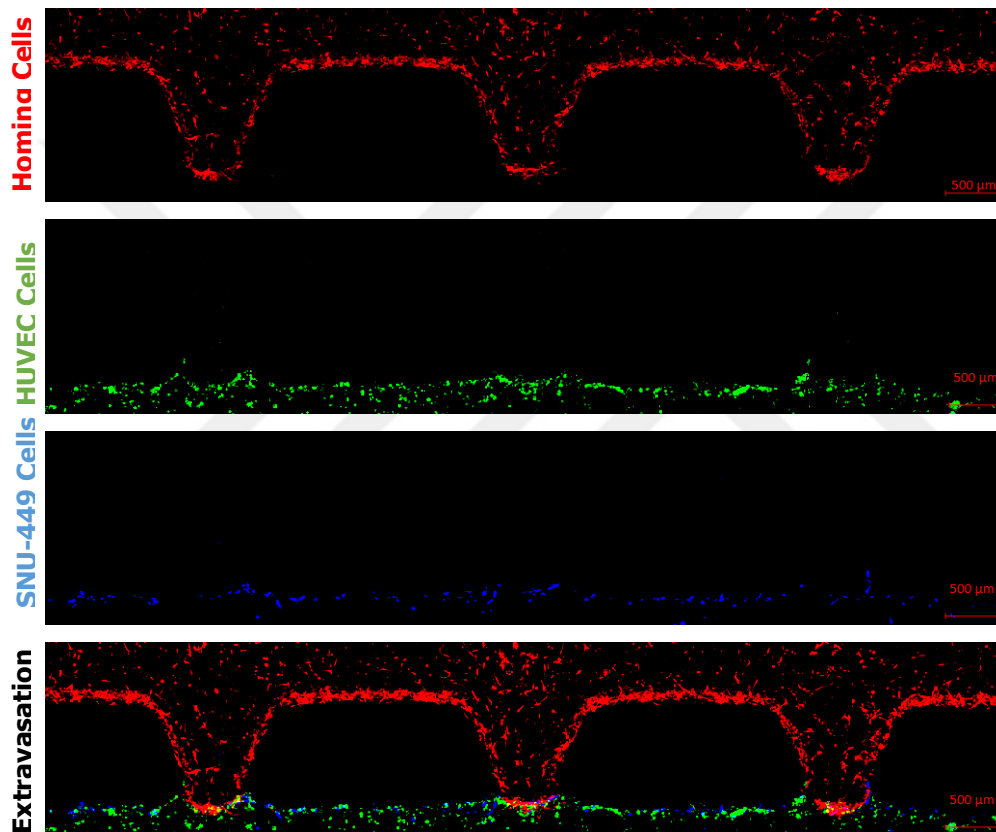


Figure 3.6 The first day image of intact extravasation LOC.

THLE-2 mCherry polyclonal homing cells in matrigel, HUVEC cells as stained with Green Cell Tracker in the flow channel to represent endothelial barrier and SNU-449 Azurite monoclonal cells in the flow channel. (The tile scan image was taken under Zeiss LSM 880, Axio Observer microscope at Izmir Biomedicine and Genome Center by using 594 nm, 488 nm and 405 nm laser and 594 nm filter, 488 nm filter and DAPI filter, under 5X objective. The image was analysed via ZEN Blue programme).

After loading of cancer cells into circulation channel, they were incubated for one week. Extravasation of cancer cells were examined under the confocal/fluorecence microscopy at day0, day2, day5 and day7. The extravazation(+) post was the passing through the endothelial barrier to reach homing target/organ. The extravasation (-) post was the staying of cancer cells

in the circulation channel and they were not passing through the endothelial barrier so as to colonize in the target organ. Fig. 3.7 indicates the extravasation (+) and extravasation (-) post respectively. The image shows the extravasation of SNU-449 Azurite monoclonal cells to HS-27A cells which was 6th days of incubation (extravasation (+)) and SNU-449 Azurite monoclonal cells were not extravasated to BEAS-2B which was 3rd days of incubation. (extravasation (-)).

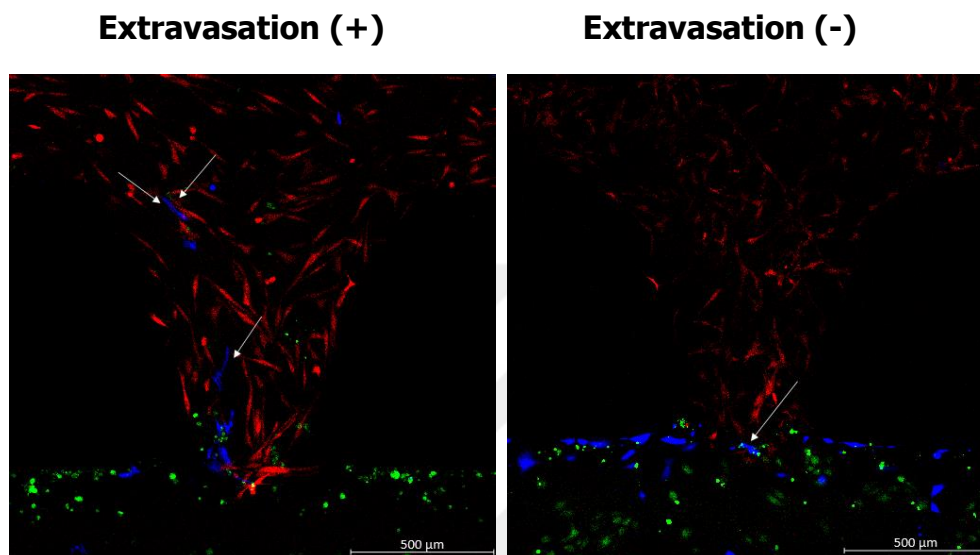


Figure 3.7 The post image of extravasation (+) and extravasation (-) for SNU-449 Azurite monoclonal cells. Extravasation of SNU-449 Azurite monoclonal cells to HS-27A (6th day for incubation) cells and the extravasation (-) image for SNU-449 cells to BEAS-2B homing cells (3rd day for incubation) for static condition. White arrow shows SNU-449 Azurite cells. (The post image was taken under Zeiss LSM 880, Axio Observer microscope at Izmir Biomedicine and Genome Center by using 594 nm, 488 nm and 405 nm laser and 594 nm filter, 488 nm filter and DAPI filter, under 5X objective. The image was analysed via ZEN Blue programme).

3.5 Extravasation of Static SNU-449 Azurite monoclonal cells which had constitively active c-Met RTK to THLE-2, BEAS-2B and HS-27A homing cells

In order to investigate the role of activation of c-Met on the organ specific extravasation static SNU-449 cells which had constitively active c-Met were loaded on the extravasation LOC which contained three different homing cells as THLE-2, BEAS-2B and HS-27A. Here, SNU-449 cells were not exposed to shear stress so they were at static condition. The extravasated post numbers were determined after 7th day incubation. The images were taken at day0, day2, day5 and day7 so as to view extravasation of SNU-449 Azurite cells to homing cells in the form of tile scan and 2D images. The extravasated posts were determined at the end of 7th day and extravasation and organ specific extravasation of SNU-449 Azurite cells was analyzed via Microsoft Excel and Graphpad Prism. Fig.3.8 shows the extravasation of SNU-449 cells to THLE-2, BEAS-2B and HS-27A homing cells respectively (Fig.3.8).

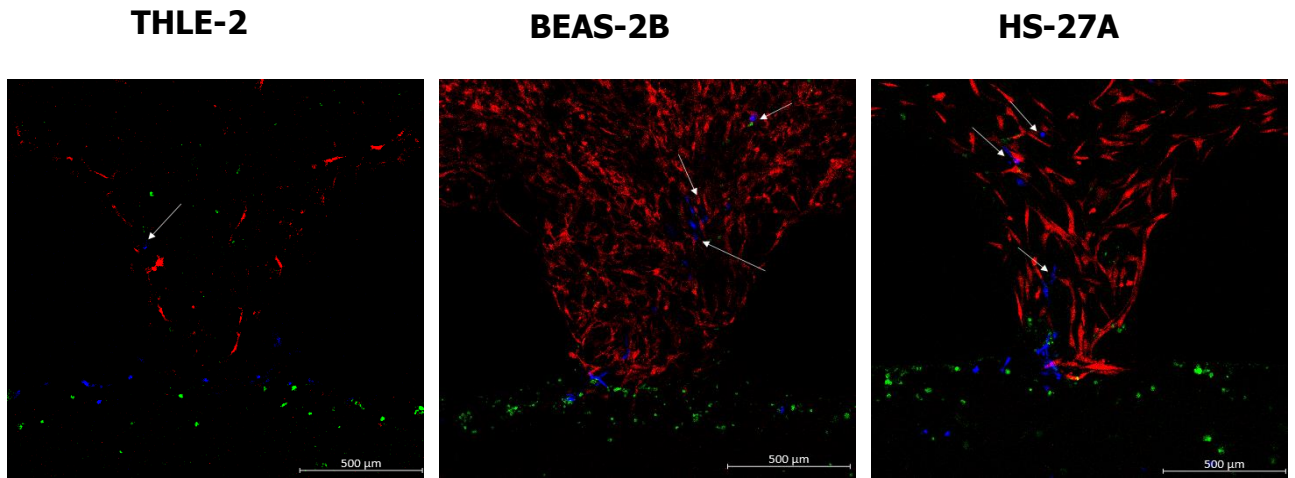


Figure 3.8 7.days images of extravasated SNU-449 Azurite monoclonal cells to THLE-2, BEAS-2B and HS-27A homing cells on the LOC respectively for static condition. White arrow shows SNU-449 Azurite cells. (The 2D images were taken under Zeiss LSM 880, Axio Observer microscope at Izmir Biomedicine and Genome Center by using 594 nm, 488 nm, 405 nm laser and 594 nm filter, 488 nm and DAPI filter under 5X objective. The image was analysed via ZEN Blue programme).

For static condition of SNU-449 cells, 85 posts were analyzed in total and they were extravasated to 40 posts of them as 47.05%. When the organ specific extravasation of SNU-449 cells were evaluated, 66.66% (20/30 post#) of them was extravasated to THLE-2 as representing liver epithelial cells, 30.76% (8/26 post#) of them were extravasated to BEAS-2B as representing lung epithelial and 41.37% (12/29 post#) of them were extravasated to HS-27A as representing bone marrow/stroma cells (Fig.3.9)

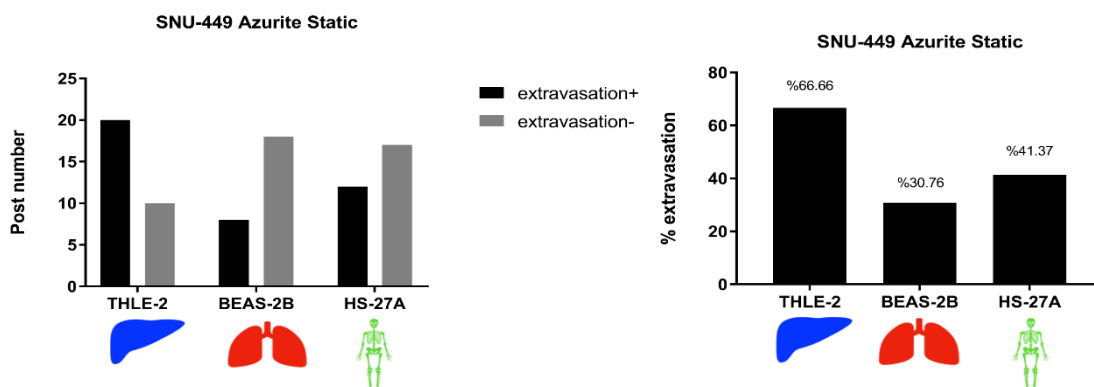


Figure 3.9 Extravasation (+) and extravasation (-) post numbers for SNU-449 cells for static condition were determined in accordance with homing organs as THLE-2, BEAS-2B and HS-27A cells after seven day incubation

(left) and the extravasation percent of each homing organ was determined by ratio of extravasated post to extravasated negativ post in itself.

In the light of this analysis, the number of total post for extravasation of SNU-449 at static condition was 40. It was determined that 20 posts of them (50%) belonged to THLE-2 liver epithelial cells, 12 posts of them (30%) belonged to HS-27A bone marrow/stroma cells and 8 posts of them (20%) belonged to BEAS-2B lung epithelial cells. Figure 3.10 indicates the percentage of organ specific extravasation of SNU-449 cells to THLE-2, HS-27A and BEAS-2B cells by pie chart at static condition.

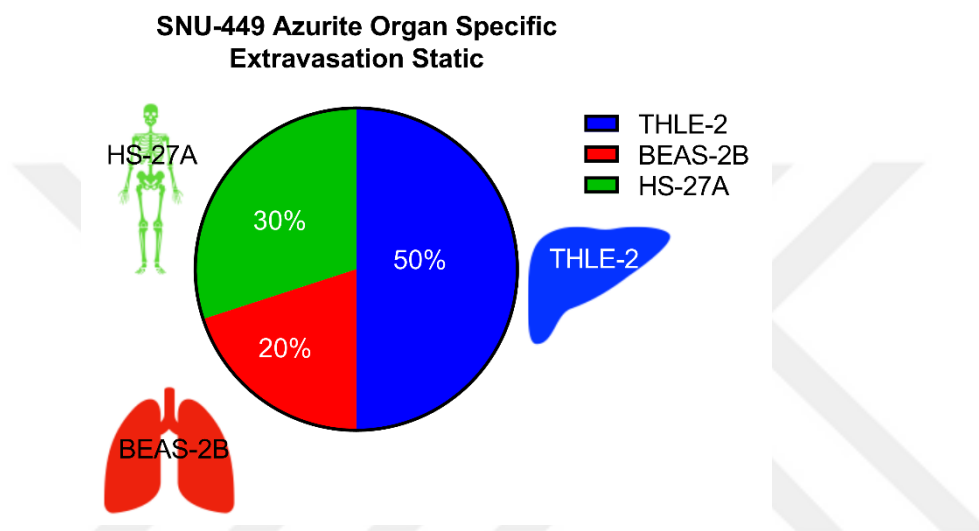


Figure 3.10 The pie chart for extravasation ratio of SNU-449 cells to THLE-2, HS-27A and BEAS-2B cells at static condition.

3.6 Inhibition c-Met RTK via SU11274 affected on extravasation frequency of SNU-449 Azurite monoclonal cells to THLE-2, BEAS-2B and HS-27A homing cells on the LOC

The organ specific extravasation of SNU-449 which had constitutively active c-Met was determined and the results were different based on different organs. Therefore, activation of c-Met was inhibited by c-Met inhibitor SU11274. The inhibition dose of SU11274 for SNU-449 cells was optimized by Atabey Laboratory as 2500 nM and this dose was used for inhibition of c-Met activation for this experiment which was described at material-method section. SNU-449 cells which were their activation of c-Met inhibited at static condition were loaded to extravasation LOCs so as to predict their organ specific extravasation. Inhibition of active c-Met caused a decrease in the extravasation of SNU-449 generally and they were not passed through the endothelial barrier and stay in the circulation channel (Fig. 3.11).

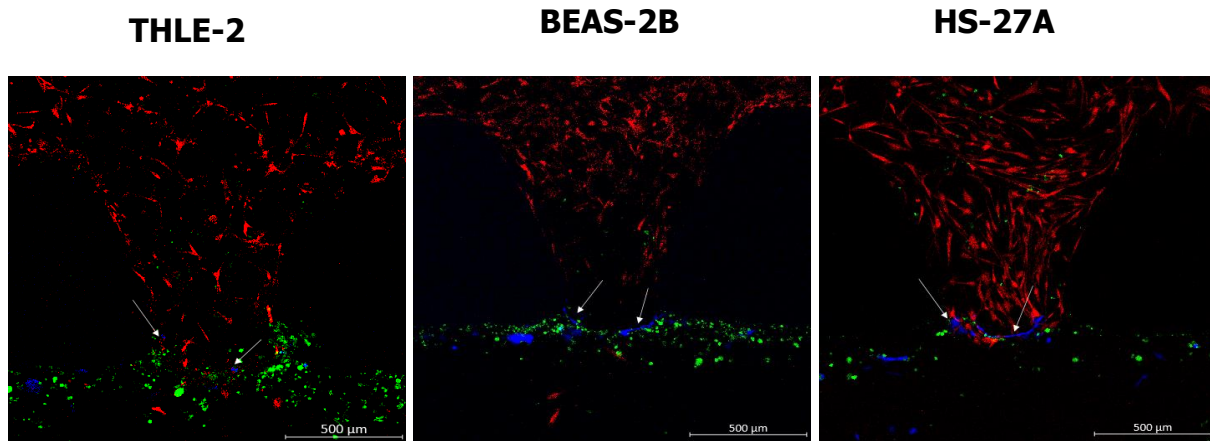


Figure 3.11 7.days images of SNU-449 Azurite monoclonal cells were treated with SU11274 to THLE-2, BEAS-2B and HS-27A homing cells on the LOC respectively for static condition. The arrow shows their location in the circulation channel and they were not passed through the HUVEC endothelial barrier. White arrow shows SNU-449 Azurite cells. (The 2D images were taken under Zeiss LSM 880, Axio Observer microscope at Izmir Biomedicine and Genome Center by using 594 nm, 488 nm, 405 nm laser and 594 nm filter, 488 nm and DAPI filter under 5X objective. The image was analysed via ZEN Blue programme).

3.7 Inhibition of activate c-Met RTK via SU12274 decreased the extravasation of SNU-449 Azurite monoclonal cells to THLE-2, BEAS-2B and HS-27A homing cells on the LOC.

The inhibition of c-Met was analysed at 149 posts in total. 64 posts of them were used for prediction of extravasation of SNU-449 cells which were treated with SU11274 and 85 posts of them were treated with DMSO as control group. The analysis was based on the extravasation results obtained at 7th day. The percent of extravasation for SNU-449 at static condition was 66.66 % (20/30 posts) for THLE-2, 30.76% (8/26) for BEAS-2B and 41.37% (12/29) for HS-27A cells. When they were treated with SU11274, the extravasation ratio was decreased generally. The percent of extravasation was 15.38% (4/26) for THLE-2, 19.04% (4/21) for BEAS-2B and 5.88% (1/17) for HS-27A cells (Fig.3.12). Treatment of SU11274 caused a decrease in the extravasation rate of SNU-449 cells as 70.12% in total. Inhibition of c-Met RTK via SU12274 decreased the extravasation rate of SNU-449 Azurite monoclonal cells to THLE-2 cells as 76.93% , to HS-27A cells as 85.79% and to BEAS-2B cells as 38.1% at static condition (Fig.3.12).

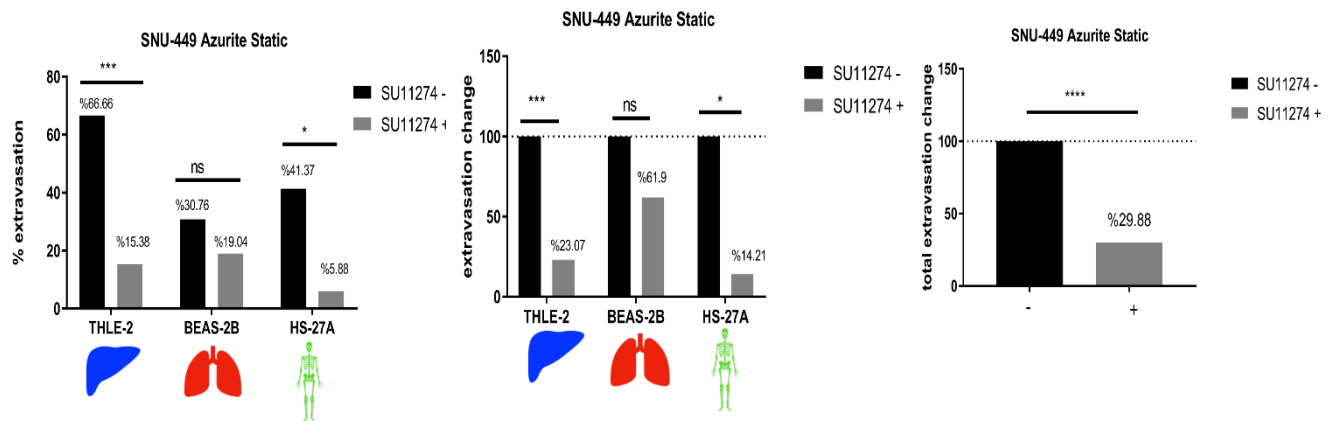


Figure 3.12 Treatment of SU11274 caused a decrease in the extravasation rate of SNU-449 cells as 70.12% in total. Inhibition of activation of c-Met RTK via SU12274 decreased the extravasation rate of SNU-449 Azurite monoclonal cells to THLE-2 cells as 76.93% and to HS-27A cells as 85.79% and to BEAS-2B cells as 38.1% at static condition. **** p<0.0001, ***p<0.001, **p<0.01, *p<0.05, Statical analyses were by Chi-square test of prospective data.

The total extravasation percent for SNU-449 cells treated with SU11274 and control group was listed at Table 3.1.

Table 3.1 The extravasation percent of SNU-449 cells treated with SU11274 and control group at static condition.

SNU-449 Static Condition		Extravasation		Total
Homing Cells	Inhibitor -/+	+	-	
THLE-2	SU11274 -	20 (%66.66)	10(%33.33)	30(%100)
	SU11274 +	4 (%15.38)	22 (%84.61)	26 (%100)
BEAS-2B	SU11274 -	8 (%30.76)	18 (%69.23)	26 (%100)
	SU11274 +	4 (%19.04)	17 (%80.95)	21 (%100)
HS-27A	SU11274 -	12 (%41.37)	17 (%58.62)	29(%100)
	SU11274 +	1 (%5.88)	16 (%94.11)	17 (%100)
Total SU11274 -		40 (%47.05)	45 (%52.94)	85 (%100)
Total SU11274 +		9 (%14.06)	55 (%85.93)	64 (%100)

3.8 Extravasation of SNU-449 Azurite monoclonal cells which were exposed to 0.5 dyn/cm² Fluid Shear Stress for 4 hours to THLE-2, BEAS-2B and HS-27A homing cells

In order to simulate the fluid shear stress exposure, peristaltic pump was used which was described at material-method section. SNU-449 cells were exposed to 0.5 dyn/cm² FSS which represented FSS for hepatic sinusoids for 4 hours. FSS exposed SNU-449 cells were loaded into LOCs and extravasation positive and negative posts were determined. Only the survival cells were loaded into the circulation channel of LOC.

The extravasated posts were determined at the end of 7th day and the post number of extravasation +/- posts was determined for each homing cells. It was determined that the percentage of extravasation was 42.85% (9/21) for THLE-2 cells, 36% (9/25) was for BEAS-2B cells and 57.89% (11/19) was for HS-27A cells (Fig.3.13).

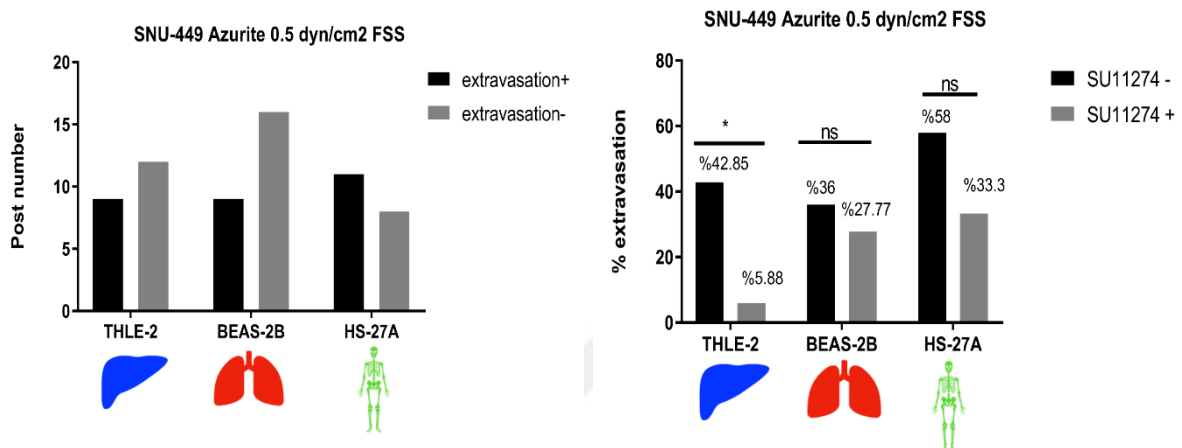


Figure 3.13 The extravasation +/- posts was determined for each homing cells for SNU-449 cells which were exposed to 0.5 dyn/cm² FSS for 4 hours based on the data obtained at 7th day after incubation and the extravasation percent of each homing organ was determined by ratio of extravasated positive post to extravasated negativ post in itself. ****p<0.0001, ***p<0.001, **p<0.01, *p<0.05, Statical analyses were by Chi-square test of prospective data.

Based on extravasation +/- post numbers, organ specific extravasation frequency of SNU-449 Azurite monoclonal cells was determined. SNU-449 cells which were exposed to FSS loaded to LOCs and 65 posts were analysed and it was determined that 29 posts of them (44.6%) were extravasation (+). 9 posts of them (31%) belonged to THLE-2, 11 posts of them (38%) belonged to HS-27A cells and 9 posts of them (31%) belonged to BEAS-2B cells (Fig.3.14).

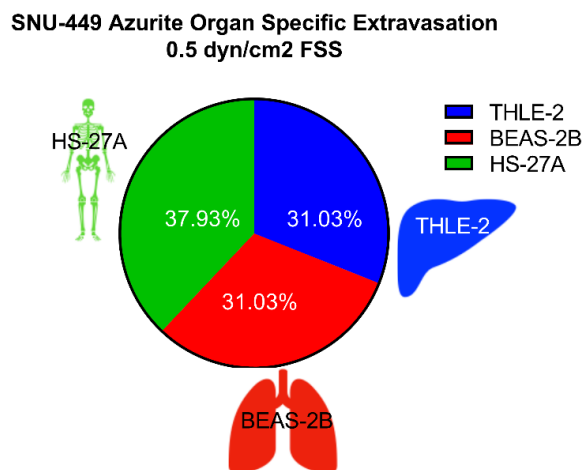


Figure 3.14 The pie chart for extravasation ratio of SNU-449 cells exposed to 0.5 dyn/cm² for 4 hours to THLE-2, HS-27A and BEAS-2B cells.

3.9 Inhibition c-Met RTK via SU11274 affected on extravasation frequency of SNU-449 Azurite monoclonal cells exposed to 0.5 dyn/cm² FSS for 4 hours to THLE-2, BEAS-2B and HS-27A homing cells on the LOC

SNU-449 cells treated with SU11274 were exposed to 0.5 dyn/cm² for 4 hours and they were loaded into LOCs so as to determine their extravasation capacity. The extravasation rate of SNU-449 cells treated with SU11274 and then exposed to 0.5 dyn/cm² FSS was decreased generally. It was determined that the percentage of extravasation was 5.88 % (1/17) for THLE-2, 27.77% (5/18) for BEAS-2B cells and 33.3% (6/18) for HS-27A cells (Fig3.15). Moreover, the total extravasation rate for homing cells was decreased 49.26% and for THLE-2 cells the rate decreased 86.24%, for BEAS-2B cells the rate decreased 22.84% and for HS-27A cells the rate decreased 42.43% (Fig.3.15).

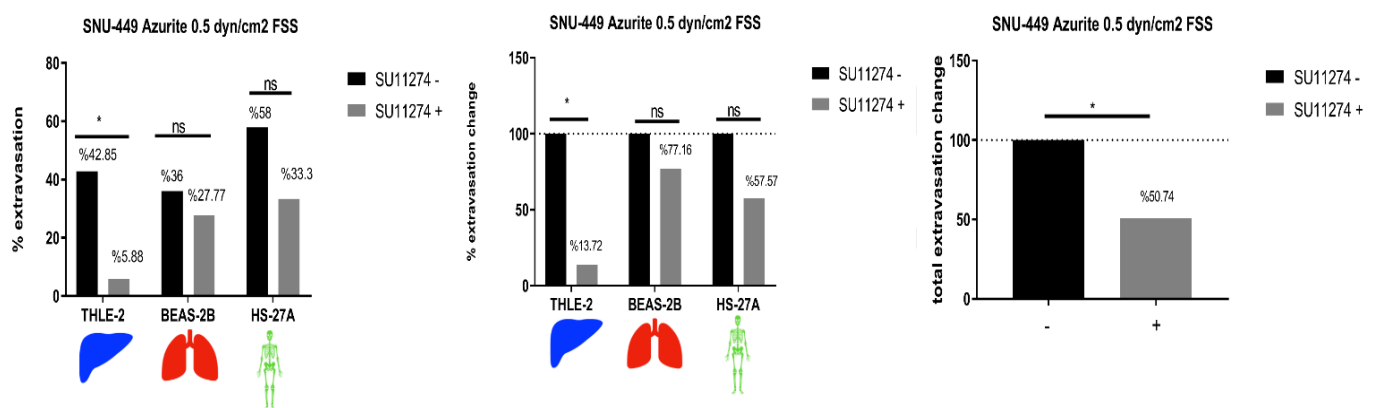


Figure 3.15 Treatment of SU11274 caused a decrease in the extravasation rate of SNU-449 cells as 49.26% in total. Inhibition of activation of c-Met RTK via SU11274 decreased the extravasation rate of SNU-449 Azurite monoclonal cells which exposed to 0.5 dyn/cm² FSS for 4 hours to THLE-2 cells as 86.24%, and to HS-27A cells as 42.43% and to BEAS-2B cells as 22.84%. ****p<0.0001, ***p<0.001, **p<0.01, *p<0.05, Statical analyses were by Chi-square test of prospective data.

The total extravasation percentage for SNU-449 cells treated with SU11274 which exposed to 0.5 dyn/cm² for 4 hours and control group was listed at Table 3.2.

Table 3.2 The extravasation percentage of SNU-449 cells treated with SU11274 which exposed to 0.5 dyn/cm² for 4 hours and control group.

0.5 dyn/cm ² FSS		Extravasation		Total
Homing Cells	Inhibitor -/+	+	-	
THLE-2	SU11274 -	9 (%42.9)	12 (%57.14)	21 (%100)
	SU11274 +	1 (%5.9)	16 (%94.11)	17 (%100)
BEAS-2B	SU11274 -	9 (%36)	16 (%64)	25 (%100)
	SU11274 +	5 (%27.77)	13 (%72.22)	18 (%100)
HS-27A	SU11274 -	11 (%57.84)	8 (%42.10)	19 (%100)
	SU11274 +	6 (%33.33)	12 (%66.66)	18 (%100)
Total SU11274 -		29 (%44.61)	36 (%55.38)	65 (%100)
Total SU11274 +		12 (%22.64)	41 (%77.35)	53(%100)

When the organ specific extravasation rate of SNU-449 cells which were exposed to 0.5 dyn/cm² FSS on the LOC was compared, they were different from the extravasation rate at static condition. The extravasation rate of SNU-449 cells were decreased 35.72% for THLE-2 cells when they were exposed to FSS and the extravasation rate of HS-27A and BEAS-2B cells was increased as 40% and 17% respectively (Fig.3.16).

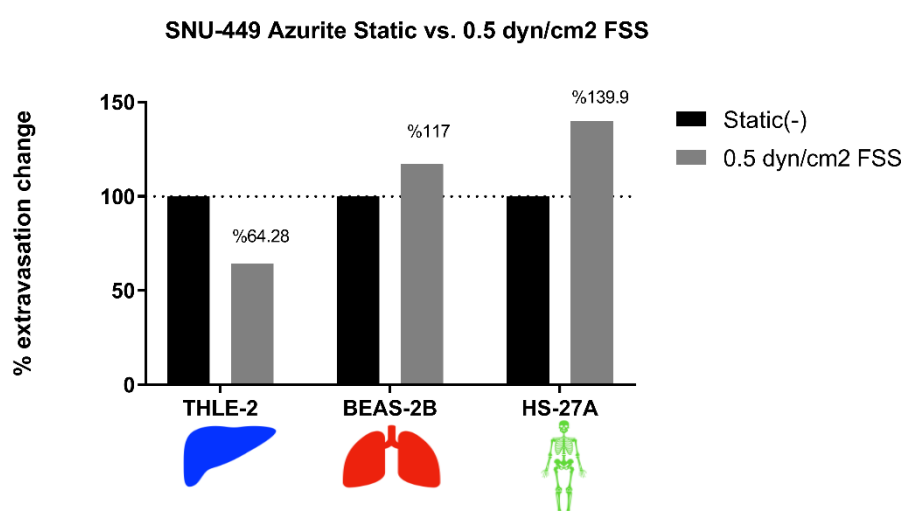


Figure 3.16 The comparison of extravasation change of SNU-449 cells at static and FSS exposed condition. The extravasation rate of SNU-449 cells were decreased 35.72% for THLE-2 cells when they were exposed to FSS and the extravasation rate of HS-27A and BEAS-2B cells was increased as 40% and 17% respectively.

3.10 Determination of Organ Specific Extravasation of SNU-398 c-Met Overexpressed Cells (SNU-398-MET-GFP)

SNU-398 cells do not have c-Met RTK and the overexpression of c-Met in these cells were performed via lentiviral approaches by Atabey Laboratory. These cells at static condition were loaded on the LOCs and the organ specific extravasation rate was determined. The extravasated posts were determined at the end of 7th day and the post number of extravasation +/- posts was determined for each homing cells. The extravasation rate of THLE-2 was 90% (9/10), 57.14% (4/7) for BEAS-2B cells and 54.5% (6/11) for HS-27A cells. The number of total post for extravasation of SNU-398 overexpressed cells at static condition was 19. It was determined that 9 posts of them (47.37%) belonged to THLE-2 liver epithelial cells, 6 posts of them (31.58%) belonged to HS-27A bone marrow/stroma cells and 4 posts of them (21.05%) belonged to BEAS-2B lung epithelial cells. Figure 3.17 indicates the extravasation +/- post number, % extravasation and percentage of organ specific extravasation of SNU-398-MET-GFP cells to THLE-2, HS-27A and BEAS-2B cells by pie chart at static condition.

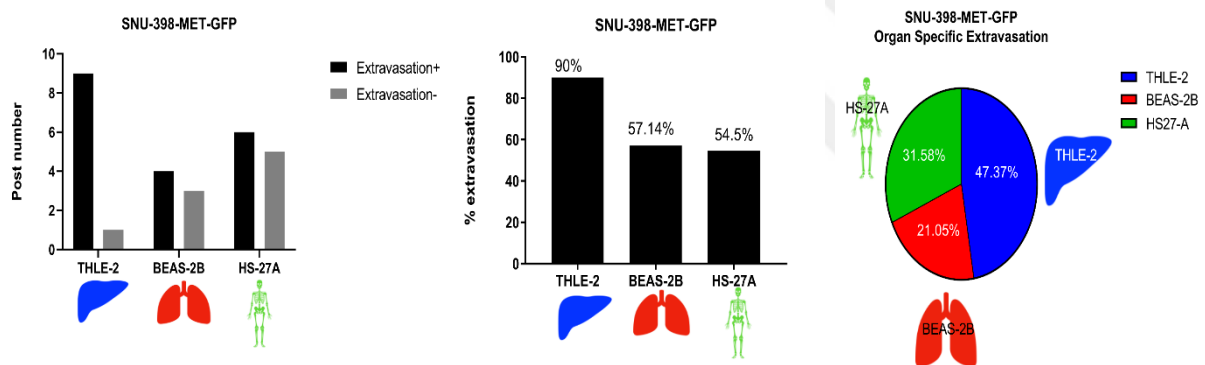


Figure 3.17 The extravasation +/- post number, % extravasation rate and the organ specific extravasation of SNU-398-MET-GFP cells by pie chart at static condition.

SNU-398 cells do not have c-Met RTK and the extravasation of SNU-398-CMV-GFP cells were determined on the LOCs. The extravasation percentage of SNU-398-CMV-GFP cells to THLE-2 was 9.1% (1/11) and to BEAS-2B cells was 40% (4/10) and to HS-27A cells was 20% (2/10). The number of total post for extravasation of SNU-398-CMV-GFP cells at static condition was 7. It was determined that 1 post of them (14.3%) belonged to THLE-2 liver epithelial cells, 2 posts of them (28.6%) belonged to HS-27A bone marrow/stroma cells and 4 posts of them (57.14%) belonged to BEAS-2B lung epithelial cells. Figure 3.18 indicates the extravasation +/- post number, % extravasation and percentage of organ specific extravasation of SNU-398-CMV-GFP cells to THLE-2, HS-27A and BEAS-2B cells by pie chart at static

condition. The presence c-Met RTK affected the extravasation of SNU-398 cells to THLE-2 liver epithelial cells significantly than the other homing cells (Fig.3.19).

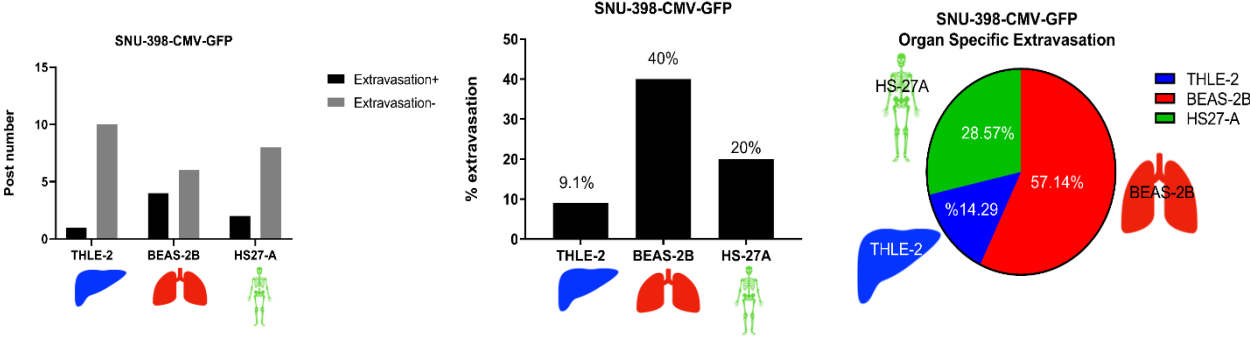


Figure 3.18 The extravasation +/- post number, % extravasation rate and the organ specific extravasation of SNU-398-CMV-GFP cells by pie chart at static condition.

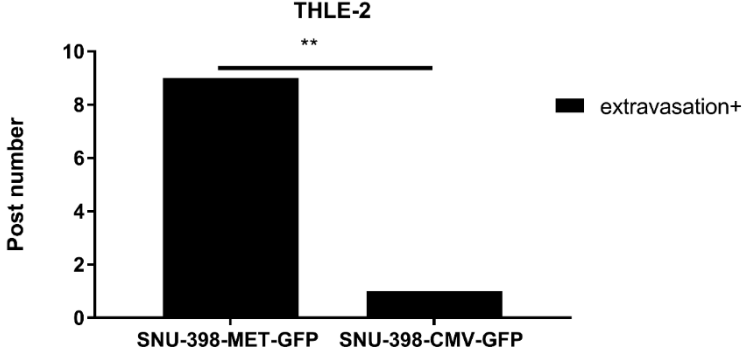


Figure 3.19 The presence or absence of c-Met RTK affected the extravasation of SNU-398 cells to THLE-2 liver epithelial cells significantly, **** p<0.0001, ***p<0.001, **p<0.01, *p<0.05, Statical analyses were by Chi-square test of prospective data.

4. DISCUSSION

Cell cultures are the most common model to investigate the role proteins in the metastasis or to understand the interaction between tumor cells and cancer cells *in vitro*. Primary cell lines which have short culture life or immortalized cell lines are used for cell cultures. Moreover, transwells are used for determination of metastatic or invasive capacity of cancer cells. They are cheaper and time-saving. However, they do not simulate *in vivo* exactly due to absence of endothelial barrier. Extravasation is one of the limiting-step of metastasis and activation of endothelium via secreted cytokines by tumor cells, NK cells or platelets recruits monocytes and facilitates the extravasation of CTCs (Labelle & Hynes, 2012). Therefore, simulation of endothelial barrier or presence of it is important. *In vitro* non-animal model is less costly on the other hand 3D cell culture model mimics *in vivo* biological systems better than 2D cell culture model (Li et al., 2012) *In silico* models are also used for metastasis studies and they are only based upon data obtained from experiments (van Marion et al., 2016). For non-animal *in vivo* studies, *Drosophila melanogaster* has common signaling pathways which play role in proliferation, invasion and motility in cancer like TGF- β pathway. Therefore, this makes *Drosophila melanogaster* as good model for cancer studies. However, Woodhouse and Liotta claimed that they were not applicable for studying angiogenesis and immune response for cancer (Woodhouse & Liotta, 2004). Due to absence of homologous organs such as liver, pancreas etc. in *Drosophila melanogaster*, some tumor types are not studied (Miles, Dyson, & Walker, 2011). Zebrafish is a useful model for cancer research and genetic studies and many genes are conserved between zebrafish and humans. Zebrafish embryos develop as *ex utero* and they are transparent until one month which enables their visualization for orthotopic xenograft transplantation studies. Moreover, at early developmental stages their immune response is not active. Therefore, there is no necessity to suppress their immune system. Some organs are absent like breast, lungs alternatively gills can be used for analogous organ. It is not applicable for big human cells due to small zebrafish organs/structures in size (Konantz et al., 2012). Animal models are also used for metastatic studies. However, immunosuppressive mice are needed for injection of human derived tumor cells to mice intravenously, subcutaneously, or orthotopically. This approach is better than *in vitro* models due to physiological suitability. However, this model is both expensive and time consuming. Absence of immune cells does not reflect biological relevance of metastasis results in treatment failure of many drugs tested on the mice for human. In addition, due to heterogeneity of tumor the response of patients to

drug is variable and is not efficient to all patients. Therefore, personalized medicine will be a correct treatment approach for cancer patients (Li et al., 2012). 3D culture systems such as organoids take into account cell-cell and cell-matrix interactions in contrast to 2D cell culture system. Coating of cell culture plates with matrix proteins still does not simulate the *in vivo*. Boyden Chamber is one of common method to study on migratory ability of cancer cells which is based upon the migration of cancer cells from upper section to lower section after passing through the pores. This method does not reflect the *in vivo* conditions due to lack of cell-cell contact, endothelium and dynamics. Recently microfluidic systems are used for metastasis and drug screening studies. Microfluidic devices is physiologically relevant to metastasis due to presence of different cell types in 3D cell culture system and they take into account biochemical, mechanical and cellular signals (Ma et al., 2018). Microfluidic system is also used to mimic metastasis of cancer cells to distant organs as liver, lung and bone (Mi et al., 2016). Metastasis is the sequential steps of dissemination of cancer cells from primary tumor to colonize secondary organs, also called as invasion-metastasis cascade (Valastyan & Weinberg, 2011). Extravasation is one limiting-step of metastasis and its mechanism is not elucidated yet. However, it is considered that is similar to leukocytes infiltration during inflammation. It consists of three steps as rolling of cancer cells through the vessel, adhesion to endothelial cells and transmigration of cancer cells. There are two hypothesis about extravasation of cancer cells, one of them is “*seed and soil*” hypothesis which is claimed that there is a specific affinity between cancer cells (seed) and microenvironment of specific organs (soil) proposed by Stephan Paget in 1889 (Zelinsky & Newman, 1974). This hypothesis is different from the hypothesis proposed by Rudolf Virchow which is the arrest of CTCs in the vessels due to size limitation of vessels (Pachmayr et al., 2017). For both hypothesis, endothelial cells are important for transmigration of cancer cells. Human umbilical cord vein cells (HUVEC) are used for mimicking of endothelial cells *in vitro*. Zhang et al. demonstrated the transmigration of adenoid cystic carcinoma (ACC) cells in the presence of chemokine CXCL12 on the lab-on-a-chip at static condition. Treatment of inhibitor AMD3100 inhibited the transmigration of adenoid cystic carcinoma (ACC) cells (Pratiti Mandal, Ranabir Dey, 2010). Moreover, breast cancer cells expressed chemokine receptor 4 (CXCR4) are migrated to the organs which possess high level of the receptor’s ligand, CXCL12 as lung, liver, bone marrow, brain(Pachmayr et al., 2017). 90% of cancer-related mortality is due to metastasis. Both frequency of the intrahepatic and extrahepatic metastasis is high in HCC (Kamimura, 2019). For primary tumor and intrahepatic metastasis; surgery, ablation and embolization treatments are administered. For extrahepatic metastasis; surgery, molecular targeted therapy are considered. Therefore,

preventing the metastasis at molecular level is very important both for intrahepatic and extrahepatic metastasis. HGF/c-Met signaling pathway is one of the essential pathway playing role in invasion, motility, cell proliferation, angiogenesis and protecting cells from apoptosis in HCC (García-Vilas & Medina, 2018). D'Amico et. al demonstrate that inhibition of c-Met on the cancer stem cells in renal tumors inhibited the bone metastasis in vivo (Godio et al., 2016). In the context of TUBITAK 1003 project #115E056 Extravasation LOCs were fabricated by Assoc. Prof. Dr. Devrim Pesen Okvur and her group at Izmir Institute of Technology (IZTECH) and the validation of these LOCs for HCC cells were performed by Prof. Dr. Neşe Atabey and her group at Izmir Biomedicine and Genome Center. In this thesis Project, Lab-on-chip device was used to mimic the extravasation of HCC cells as SNU-449 having constitively active c-Met and SNU-398 cells which absent c-Met in 3D cell culture system to investigate the role of c-Met on the organ specific extravasation. LOC is composed of three channels as medium channel, homing channel and circulation channel. Homing cells were THLE-2 as representing liver epithelial cells, HS-27A as representing bone marrow/stroma cells and BEAS-2B as representing lung epithelial cells. HUVEC cells were used to mimic the endothelial barrier and SNU-449 and SNU-398 cells are used to simulate the circulating tumor cells having constitively active c-Met or lack of c-Met. All cells had fluorescence proteins so as to easily visualized extravasation of cancer cells under fluorescence and confocal microscope. In this study, it was aimed that to investigate the role c-Met activation in the organ specific extravasation in HCC cells. Therefore, SNU-449 cells which had constitively active c-Met and SNU-398 cells which was lack of c-Met were used and these cells were loaded into the LOCs at static and 0.5 dyn/cm² Fluid shear stress (FSS) exposed conditions. FSS is force of friction between dynamic layer in steady flow. FSS leads to killing of CTCs apart from NK cells, immune cells. Only %0.02 of CTCs is able to form metastases even though millions of CTCs are circulated every day. Therefore, loading of FSS exposed cells to the LOCs was physiologically relevant to *in vivo*. The proliferation capacity and viability of these cells were determined by MTT assay and trypan blue respectively in parallel to loading of them the LOCs (data not shown). Exposure to FSS decreased their proliferation capacity significantly when SNU-449 at static DMSO condition was compared with 0.5 dyn/cm² FSS exposed condition for 4 hours or SNU-449 treated with SU11274 at static condition with SNU-449 treated with SU11274 exposed to 0.5 dyn/cm² FSS for 4 hours. The FSS in hepatic sinusoid is between 0.1dyn/cm² and 0.5 dyn/cm² and therefore the HCC cell lines exposed to 0.5 dyn/cm² FSS for 4 hours which was optimized. Extravasation rate of SNU-449 cells was different at static condition and FSS exposed condition. Figure 3.16 shows that the extravasation rate of SNU-449 cells were decreased 35.72% for THLE-2 cells

when they were exposed to FSS and the extravasation rate of HS-27A and BEAS-2B cells was increased as 40% and 17% respectively. Extravasation percentage of SNU-449 at static condition was 50% to THLE-2, 30% to HS-27A and 20% to BEAS-2B cells (Fig.3.10). This results correlated with clinical findings. The most common reason cancer-associated mortality in HCC is due to high recurrence and metastasis risk (Kamimura, 2019). Becker et al., 2014 claimed that the rate of extrahepatic metastatic sites were lungs (55%), lymph nodes (53%), bone (28%), adrenal glands (11%), peritoneum and/or omentum (11%), and brain (2%) (Becker et al., 2014). Moreover, the LOCs were used in this study for drug screening such as treatment of c-Met inhibitor SU11274 to inhibit the extravasation of SNU-449 cells. SNU-449 cells were treated with SU11274 overnight and they were loaded into the LOCs to predict their extravasation to homing cells at static condition. Figure 3.12 indicates that treatment of SU11274 decreased the extravasation rate of SNU-449 cells as 70.12% in total. Inhibition of c-Met RTK via SU12274 decreased the extravasation rate of SNU-449 Azurite monoclonal cells to THLE-2 cells as 77%, to HS-27A cells as 85.8% and to BEAS-2B cells as 38.1% at static condition. This data demonstrated that activation of c-Met could play role in organ specific extravasation especially in intrahepatic metastasis. This results demonstrated that extravasation LOC could be used for anticancer drug screening. The extravasation rate of SNU-449 cells treated with SU11274 overnight and then exposed to 0.5 dyn/cm² FSS decreased generally when compared to FSS exposed control group. The total extravasation rate for homing cells decreased 49.3% and for THLE-2 cells the rate decreased 86%, for BEAS-2B cells the rate decreased 23% and for HS-27A cells the rate decreased 42%. Extravasation rate of SNU-449 cells treated with SU11274 at static condition was different from 0.5 dyn/cm² FSS exposed condition. The extravasation LOC combined different cell types like homing cells as THLE-2/BEAS-2B/HS-27A, HUVEC cells as endothelial cells and cancer cells as SNU-449, SNU-398 in the same 3D microenvironment and in the presence of biochemical, mechanical forces on a single device. This showed that the role of mechanical force in the extravasation and the LOCs could be used for predicting the homing capacity of cancer cells. SNU-398 cells did not have c-Met expression and the overexpression of c-Met in these cells were performed by transduction. Extravasation percentage of SNU-398-MET-GFP at static condition was 47.37% to THLE-2, 31.58% to HS-27A and 21.05% to BEAS-2B cells in Figure 3.17. This results were very similar to the results obtained from extravasation percentage of SNU-449 at static condition in the Figure 3.10. SNU-398 cells did not have c-Met expression/activation and the extravasation of SNU-398-CMV-GFP cells were determined on the LOCs to investigate the role of c-Met on the organ specific extravasation. The pie chart on the Figure 3.18 shows

extravasation percentage of SNU-398-CMV-GFP at static condition is 14.3% to THLE-2, 28.6% to HS-27A and 57.14% to BEAS-2B cells. The overexpression c-Met affected the extravasation of SNU-398 cells to THLE-2 liver epithelial cells significantly than the other homing cells (Fig.3.19). The results obtained from organ specific extravasation of SNU-398-MET-GFP and SNU-398-CMV-GFP cells indicated that activation of c-Met could play role in organ specific extravasation especially in intrahepatic metastasis and bone metastasis.



5. CONCLUSION

- 1) The results obtained from the developed device as extravasation LOC indicated that the LOC could be used for to determine the extravasation of capacity of HCC cells. It is necessary to test the organ preference of circulating tumor cells (CTCs) isolated from HCC developed patients on the extravasation LOC.
- 2) Activation of c-Met could play role in organ specific extravasation especially in intrahepatic metastasis and bone metastasis. Treatment of SU11274 caused a decrease in the extravasation rate of SNU-449 cells as 70.12% in total at static condition and as 49.26% in total at 0.5 dyn/cm² FSS exposed condition.
- 3) Extravasation percentage of SNU-398-MET-GFP at static condition was 47.37% to THLE-2, 31.58% to HS-27A and 21.05% to BEAS-2B cells. This results were very similar to the results obtained from extravasation percentage of SNU-449 which had constitively active c-Met at static condition.
- 4) Exposure of SNU-449 cells to 0.5 dyn/cm² FSS increased the activation of c-Met which increased their extravasation rate in parallel. The extravasation rate of SNU-449 cells were decreased 35.72% for THLE-2 cells when they were exposed to FSS and the extravasation rate of HS-27A and BEAS-2B cells was increased as 40% and 17% respectively.
- 5) From which it's concluded that, SU11274 can be used as anti-cancer drug to prevent metastasis especially to prevent liver cancer and can be used for therapeutic purposes.

6. PERSPECTIVES

For future perspectives,

- 1) Circulating tumor cells (CTCs) will planned to be isolated from HCC developed patients. After, enrichment of these CTCs the organ preference of CTCs is planned to be predicted via extravasation LOC. Moreover, characterization of these CTCs in terms of c-Met activation is planned to be done.
- 2) The conditioned medium on the homing cells as THLE-2, HS-27A, BEAS-2B is planned to be collected and ELISA for candidate molecules is planned to be done so as to determine their level in the supernatant of homing cells and the investigate whether there is a correlation between expression of candidate molecule level and organ specific extravasation in terms of c-Met activation/expression level in HCC cells.

7. REFERENCES

- Aravalli, R. N., Cressman, E. N. K., & Steer, C. J. (2013). Cellular and molecular mechanisms of hepatocellular carcinoma: An update. *Archives of Toxicology*, 87(2), 227–247. <https://doi.org/10.1007/s00204-012-0931-2>
- Balogh, J., Iii, D. V., Gordon, S., Li, X., Ghobrial, R. M., & Jr, H. P. M. (2016). *Jhc-3-041*. 41–53. <https://doi.org/https://doi.org/10.2147/JHC.S61146>
- Becker, A. K., Tso, D. K., Harris, A. C., Malfair, D., & Chang, S. D. (2014). Extrahepatic metastases of hepatocellular carcinoma: A spectrum of imaging findings. *Canadian Association of Radiologists Journal*, 65(1), 60–66. <https://doi.org/10.1016/j.carj.2013.05.004>
- Brown, D. M., & Ruoslahti, E. (2004). Metadherin, a cell surface protein in breast tumors that mediates lung metastasis. *Cancer Cell*, 5(4), 365–374. [https://doi.org/10.1016/S1535-6108\(04\)00079-0](https://doi.org/10.1016/S1535-6108(04)00079-0)
- Farazi, P. A., & DePinho, R. A. (2006). Hepatocellular carcinoma pathogenesis: From genes to environment. *Nature Reviews Cancer*, 6(9), 674–687. <https://doi.org/10.1038/nrc1934>
- García-Vilas, J. A., & Medina, M. Á. (2018). Updates on the hepatocyte growth factor/c-Met axis in hepatocellular carcinoma and its therapeutic implications. *World Journal of Gastroenterology*, 24(33), 3695–3706. <https://doi.org/10.3748/wjg.v24.i33.3695>
- Godio, L., Belisario, D., Carbonare, L. D., Bussolati, B., Dalmaso, E., Comoglio, P., ... Migliardi, G. (2016). C-met inhibition blocks bone metastasis development induced by renal cancer stem cells. *Oncotarget*, 7(29). <https://doi.org/10.18632/oncotarget.9997>
- Guo, W., & Giancotti, F. G. (2004). Integrin signalling during tumour progression. *Nature Reviews Molecular Cell Biology*, 5(10), 816–826. <https://doi.org/10.1038/nrm1490>
- Gupta, G. P., & Massagué, J. (2006). Cancer Metastasis: Building a Framework. *Cell*, 127(4), 679–695. <https://doi.org/10.1016/j.cell.2006.11.001>
- Hsieh-Fu, T., Alen, T., Q., S. A., & Gang, B. (2017). Tumour-on-a-chip: microfluidic models of tumour morphology, growth and microenvironment. *Journal of The Royal Society Interface*, 14(131), 20170137. <https://doi.org/10.1098/rsif.2017.0137>
- Huang, Q., Hu, X., He, W., Zhao, Y., Hao, S., Wu, Q., ... Shi, M. (2018). Fluid shear stress and tumor metastasis. *American Journal of Cancer Research*, 8(5), 763–777. Retrieved from <http://www.ncbi.nlm.nih.gov/pubmed/29888101> <http://www.pubmedcentral.nih.gov/articlerender.fcgi?artid=PMC5992512>

- Kamimura, K. (2019). Identification of molecular transition of hepatocellular carcinoma: a novel method to predict the initiation of metastasis. *Stem Cell Investigation*, 6, 5–5. <https://doi.org/10.21037/sci.2019.02.02>
- Konantz, M., Balci, T. B., Hartwig, U. F., Dellaire, G., André, M. C., Berman, J. N., & Lengerke, C. (2012). Zebrafish xenografts as a tool for in vivo studies on human cancer. *Annals of the New York Academy of Sciences*, 1266(1), 124–137. <https://doi.org/10.1111/j.1749-6632.2012.06575.x>
- Kong, J., Luo, Y., Jin, D., An, F., Zhang, W., Liu, L., ... Liu, T. (2016). A novel microfluidic model can mimic organ-specific metastasis of circulating tumor cells. *Oncotarget*, 7(48). <https://doi.org/10.18632/oncotarget.9382>
- Labelle, M., & Hynes, R. O. (2012). The initial hours of metastasis: The importance of cooperative host-tumor cell interactions during hematogenous dissemination. *Cancer Discovery*, 2(12), 1091–1099. <https://doi.org/10.1158/2159-8290.CD-12-0329>
- Li, Y., Tang, Z. Y., & Hou, J. X. (2012). Hepatocellular carcinoma: Insight from animal models. *Nature Reviews Gastroenterology and Hepatology*, 9(1), 32–43. <https://doi.org/10.1038/nrgastro.2011.196>
- Ma, Y.-H. V., Middleton, K., You, L., & Sun, Y. (2018). A review of microfluidic approaches for investigating cancer extravasation during metastasis. *Microsystems & Nanoengineering*, 4(1), 1–13. <https://doi.org/10.1038/micronano.2017.104>
- Malandrino, A., Kamm, R. D., & Moeendarbary, E. (2018). In Vitro Modeling of Mechanics in Cancer Metastasis. *ACS Biomaterials Science and Engineering*, 4(2), 294–301. <https://doi.org/10.1021/acsbiomaterials.7b00041>
- Massagué, J., & Obenauf, A. C. (2016). Metastatic colonization by circulating tumour cells. *Nature*, 529(7586), 298–306. <https://doi.org/10.1038/nature17038>
- Mi, S., Du, Z., Xu, Y., Wu, Z., Qian, X., Zhang, M., & Sun, W. (2016). Microfluidic co-culture system for cancer migratory analysis and anti-metastatic drugs screening. *Scientific Reports*, 6(June), 1–11. <https://doi.org/10.1038/srep35544>
- Mierke, C. T. (2008). Role of the Endothelium during Tumor Cell Metastasis: Is the Endothelium a Barrier or a Promoter for Cell Invasion and Metastasis? *Journal of Biophysics*, 2008, 1–13. <https://doi.org/10.1155/2008/183516>
- Miles, W. O., Dyson, N. J., & Walker, J. A. (2011). Modeling tumor invasion and metastasis in *Drosophila*. *Disease Models & Mechanisms*, 4(6), 753–761. <https://doi.org/10.1242/dmm.006908>
- Mo, H.-N., & Liu, P. (2017). Targeting MET in cancer therapy. *Chronic Diseases and*

- Translational Medicine*, 3(3), 148–153. <https://doi.org/10.1016/j.cdtm.2017.06.002>
- NAKAMURA, T., & MIZUNO, S. (2010). The discovery of Hepatocyte Growth Factor (HGF) and its significance for cell biology, life sciences and clinical medicine. *Proceedings of the Japan Academy, Series B*, 86(6), 588–610. <https://doi.org/10.2183/pjab.86.588>
- Obenauf, A. C., & Massagué, J. (2016). *Surviving at a distance : organ specific metastasis*. 1(1), 76–91. <https://doi.org/10.1016/j.trecan.2015.07.009>.Surviving
- Organ, S. L., & Tsao, M. S. (2011). An overview of the c-MET signaling pathway. *Therapeutic Advances in Medical Oncology*, 3(1), S7–S19. <https://doi.org/10.1177/1758834011422556>
- Pachmayr, E., Treese, C., & Stein, U. (2017). Underlying Mechanisms for Distant Metastasis - Molecular Biology. *Visceral Medicine*, 33(1), 11–20. <https://doi.org/10.1159/000454696>
- Playford, M. P., & Schaller, M. D. (2004). The interplay between Src and integrins in normal and tumor biology. *Oncogene*, 23(48 REV. ISS. 7), 7928–7946. <https://doi.org/10.1038/sj.onc.1208080>
- Pratiti Mandal, Ranabir Dey, S. C. (2010). Lab on a Chip Lab on a Chip. *Lab on a Chip*, (207890), 531–540. <https://doi.org/10.1039/C5LC00716J>
- Schlesinger, M. (2018). Role of platelets and platelet receptors in cancer metastasis. *Journal of Hematology & Oncology*, 11(1), 1–15. <https://doi.org/10.1186/s13045-018-0669-2>
- Singh, A. K., Kumar, R., & Pandey, A. K. (2018). Hepatocellular Carcinoma: Causes, Mechanism of Progression and Biomarkers. *Current Chemical Genomics and Translational Medicine*, 12(1), 9–26. <https://doi.org/10.2174/2213988501812010009>
- Sleeboom, J. J. F., Eslami Amirabadi, H., Nair, P., Sahlgren, C. M., & den Toonder, J. M. J. (2018). Metastasis in context: modeling the tumor microenvironment with cancer-on-a-chip approaches. *Disease Models & Mechanisms*, 11(3), dmm033100. <https://doi.org/10.1242/dmm.033100>
- Steeg, P. S. (2006). Tumor metastasis: Mechanistic insights and clinical challenges. *Nature Medicine*, 12(8), 895–904. <https://doi.org/10.1038/nm1469>
- Valastyan, S., & Weinberg, R. A. (2011). Tumor metastasis: Molecular insights and evolving paradigms. *Cell*, 147(2), 275–292. <https://doi.org/10.1016/j.cell.2011.09.024>
- van Marion, D. M. S., Domanska, U. M., Timmer-Bosscha, H., & Walenkamp, A. M. E. (2016). Studying cancer metastasis: Existing models, challenges and future perspectives. *Critical Reviews in Oncology/Hematology*, 97, 107–117.

<https://doi.org/10.1016/j.critrevonc.2015.08.009>

Whittaker, S., Marais, R., & Zhu, A. X. (2010). The role of signaling pathways in the development and treatment of hepatocellular carcinoma. *Oncogene*, 29(36), 4989–5005.

<https://doi.org/10.1038/onc.2010.236>

Woodhouse, E. C., & Liotta, L. A. (2004). *Drosophila* invasive tumors: A model for understanding metastasis. *Cell Cycle*, 3(1), 38–40. <https://doi.org/10.4161/cc.3.1.636>

Zelinsky, W., & Newman, J. L. (1974). Hypothesis Revisited. *Annals of the Association of American Geographers*, 64(1), 185–187. Retrieved from

<http://www.jstor.org/stable/2562207>



8. APPENDIX

CHIP NAME					
COATING& Notes(any leak, blockage etc.)					
DEHUMIDIFICATION					
Drying date				Notes	
Experiment date:					
Cells		Label (+/-)		Notes	
Homing cells					
HCC cells					
HUVEC cells					
CTC cells					
FOLLOWING					
Bright field Control's Notes					
Date	Notes(bubbles,medium, matrigel shrinkage etc.)				
	Post 1	Post2	Post3	Post4	Post5
D					
D					
D					
Medium Change					
Date	Note;				
	Post 1	Post2	Post3	Post4	Post5
D					
D					
Confocal image					
Date 0h	Note;				
	Post 1	Post2	Post3	Post4	Post5
Tilescan					
2D					
Z-stack					
Date 48h	Note;				
	Post 1	Post2	Post3	Post4	Post5
Tilescan					
2D					
Z-stack					
Date 5.day	Note;				
	Post 1	Post2	Post3	Post4	Post5
Tilescan					
2D					
Z-stack					
Date 7.day	Note;				
	Post 1	Post2	Post3	Post4	Post5
Tilescan					
2D					
Z-stack					

9. CURRICULUM VITAE (CV)

PERSONAL INFORMATION GÜLSÜN BAĞCI

Address: Izmir Biomedicine and Genome Center (IBG),
Dokuz Eylul University Health Campus,
Mithatpasa St. No: 58/5, Balçova 35340, Izmir/TURKEY

E-mail address: gulsun.bagci@msfr.ibg.edu.tr, gulsunbagci65@gmail.com,

Mobile Phone: +90553 869 6607

Date of Birth: 24/06/1993

EDUCATION:

2016- 2019: MSc in Molecular Biology and Genetics
Dokuz Eylul University,
Izmir International Biomedicine and Genome Institute (IBG)
Molecular Biology and Genetics Department
GPA:3,88/4,00

2012-2016: BSc in Molecular Biology and Genetics
Izmir Institute of Technology (IZTECH)
Molecular Biology and Genetics Department
GPA:3,22/4,00

2011-2012: English Preparation School
Izmir Institute of Technology (IZTECH), School of Foreign Languages

Research Experience :

22/01/2016-12/02/2016: Internship at iBG
Laboratory of Cancer Biology and Signaling, Dokuz Eylul University,
Izmir Biomedicine and Genome Center (IBG), Prof. Dr. Neşe Atabey

22/06/2015-18/09/2015: Internship at KU Leuven
Laboratory of Cellular Metabolism and Metabolic Regulation KU Leuven VIB
Vesalius Research Center, Leuven/Belgium, Assist. Prof. Dr. Sarah Maria Fendt

07/2014-02/2015: Internship at IZTECH
Breast Cancer Laboratory, Izmir Institute of Technology (IZTECH),
Molecular Biology and Genetics Department, Assist. Prof. Dr. Özden Yalçın
Özuysal

Personal Skills

Language: Turkish (native), English (advance), French (basic)

Computer Skills:

Bioinformatics tools, MS Office Applications, C programming, KNIME, Microsoft Access

Congress Participated:

21/02/2019-23/02/2019:
3rd Çukurova Congress of Hepatocellular Carcinoma, Sheraton Grand

Adana, Adana/Turkey

5/09/2018-8/09/2018:

6th International Congress of the Molecular Biology Association of Turkey, iBG-Izmir, Izmir/Turkey

11/11/2017: Therapeutic mAb Engineering and Production Certification Workshop, Dokuz Eylul University, Izmir Biomedicine and Genome Center (IBG)

10/11/2017: New Frontiers in Life Sciences Symposium, Dokuz Eylul University, Izmir Biomedicine and Genome Center (IBG)

23/04/2017-26/04/2017:

EMBO Metabolic Disorders and Liver Cancer, Palma de Mallorca/Spain

PRACTISED LABORATORY METHOD: Cell Culture Techniques, Real-time-qPCR, Cloning, Western Blot, Annexin V method, Sulforhodamine B colorimetric assay, Invazyon/Motility Assays, Tubulogenesis, IF, PBMC isolation and CTC culturing, 3D culture experiment (Lab-on-a-chip device), spheroid/invasion, co-culture experiment, MTT, Confocal and fluorescence imaging techniques.

Research Experience

Master Thesis

2016-2019: The Role of c-Met Activation on the Organ Specific Extravasation in Hepatocellular Carcinoma Cells, Izmir International Biomedicine and Genome Institute (iBG), Dokuz Eylul University

2016-2019:Project:

A Novel Lab-on-a-Chip Device for Early Diagnosis of Metastasis
Dokuz Eylul University, Supported by: TUBITAK

2016-2017: Project:

Molecular Mechanism of High Glucose Induced Hepatocellular Carcinoma Progression: c-Met Activation and New Players Thioredoxin Interacting Protein, Sestrin2 and lncRNA HOTAIR

Dokuz Eylul University Supported by: TUBITAK

Certifications:

Certificate of Experimental Animal Usage for Researchers, Dokuz Eylul University, 2017

Certificate of Awareness, Research and Literacy of Patent, Yalçiner Patent,2019

Thesis: Bagci G., (2019). *The Role of c-Met Activation in the Organ Specific Extravasation in HCC Cells (Master Dissertation)*. Izmir International Biomedicine and Genome Institute, Izmir, Turkey.

Poster Presentation

Poster: Bagci G., Comez D, Bagirsakci E, Topel H, Yilmaz Y, Gunes A, Batı Ayaz G, Pesen Okvur D, Atabey N. *HCC Hücrelerinde Organ Spesifik Metastazda C-Met Yolağı Rolünün Yonga Üstü Laboratuvar Cihazı Kullanılarak İncelenmesi*, 3th Çukurova Congress of Hepatocellular Carcinoma, 2019, Adana, Turkey.

Poster: Topel H, Yilmaz Y, Gunes A, Bagirsakci E, Gizem BA, Comez D, **Bagci G,** Kahraman E, Pesen Okvur D, Atabey N. *Predicting homing ability of hepatocellular carcinoma cells by using a lab-on-a-chip system*, EACR25: 25th Biennial Congress of the European Association for Cancer Research, 2018, Amsterdam, Netherlands.

Oral Presentation

Comez D, Bagci G., Topel H, Bagirsakci E, Yilmaz Y, Gunes A, Atabey N. *c-Met aktivasyonunun Hepatoselüler Karsinoma Hücrelerinin Sıvı Teğetsel Gerilme Stresinde Sağkalımına ve Metastatik Kapasitesine Etkisi*, 3th Çukurova Congress of Hepatocellular Carcinoma, 2019, Adana, Turkey.

Academic Reference

- 1) Prof. Dr. Nese ATABEY, Laboratory of Cancer Biology and Signalling Izmir Biomedicine and Genome Center (IBG) Dokuz Eylul University Health Campus, Mithatpasa St. No: 58/5, Balçova 35340 Izmir / TURKEY. Phone number: +905055250207, Email: nese.atabey@ibg.edu.tr
- 2) Assistant Professor Dr. Sarah Maria Fendt, Laboratory of Cellular Metabolism and Metabolic Regulation KU Leuven VIB Vesalius Research Center, Leuven, Belgium, Campus Gasthuisberg O&N4 Herestraat 49, box 912 3000 Leuven, Belgium, Office Phone :+32 16 37 32 35, Email : sarah-maria.fendt@vib-kuleuven.be
- 3) Assistant Professor Dr. Özden Yalçın Özuysal Department Of Molecular Biology and Genetics Izmir Institute of Technology 35430, Urla, Izmir, TURKEY Office Phone: +90 232 750 7311, Email: ozdenyalcin@iyte.edu.tr

